Designing of Computer Aided Diagnostic System for the Identification of Exudates in Retinal Fundus Image

A Dissertation submitted in fulfillment of the requirements for the Degree

of

MASTER OF ENGINEERING

in

Electronic Instrumentation & Control Engineering

Submitted by:

SANTOSH KUMAR MISHRA

Regd.No. (801351024)

Under the guidance of

Dr Deepti Mittal

(Assistant Professor, EIED)

2015

Electrical and Instrumentation Engineering Department

Thapar University, Patiala

(*Declared as Deemed-to-be-university u/s 3of the UGC Act.,1956*)

Post Bag No 32, Patiala – 147004

Punjab (India)

DECLARATION

I hereby certify that the work which is presented in dissertation entitled, "Designing of Computer Aided Diagnostic System for the Identification of Exudates in Retinal Fundus Images", in partial fulfillment of the requirements for the award of the degree of Master of Engineering in Electronics Instrumentation and Control Engineering, submitted to Electrical & Instrumentation Engineering Department of Thapar University, Patiala is as authentic record of my own work carried under the supervision of Dr Deepti Mittal. It refers others researcher's work which are duly listed in the reference section. The matter contained in this dissertation has not been submitted, neither in part nor in full to any other degree to any other university or institute except as reported in text and references.

Santosh Kumar Mishra

Place: Patiala
Date: 15/07/2015

Santosh Kumar Mishra
Roll No.: 801351024

It is certified that the above statement made by the student is correct to the best of my knowledge and belief.

Date: 15/07/2015

Dr Deepti Mittal
Assistant Professor
Electrical & Instrumentation Engineering Department
Thapar University, Patiala

Countersigned by:

Head
Electrical & Instrumentation Engineering Department
Thapar University, Patiala

Dean (Academic Affairs)
Thapar University, Patiala

ACKNOWLEDGEMENT

I would like to take the opportunity to express my gratitude to some people who were involved in this dissertation work. First, I owe my gratitude to my mentor Dr. Deepti Mittal for doing everything from the inception of the project idea to giving invaluable suggestions at every step.

I am also thankful to Dr. Ravinder Agarwal, Head of the Department and Mr. Nirbhow jap singh PG Coordinator as well as all the faculty members and staff of the Electrical and Instrumentation Engineering Department for being very supportive to me. I would also like to thank all my batch mates for motivating me all the time whenever I needed them and giving me useful tips. I thank all those who have contributed directly or indirectly to this work.

Lastly, I would also like to thank my parents for their years of unyielding love and encourage. They have always wanted the best for me and I admire their determination and sacrifice.

Santosh Kumar Mishra

SANTOSH KUMAR MISHRA

801351024

iii

TABLE OF CONTENT

TABLE OF CONTENTS (Continued)

LISTS OF FIGURE

LIST OF TABLE

ABBREVIATIONS

OCT	Optical Coherent Tomography
DR	Diabetic Retinopathy
DME	Diabetic Macular Edema
Non-CSME	Non-Clinically Significant Macular Edema
CSME	Clinically Significant Macular Edema
AMD	Age–Related Macular Degeneration
CNV	Choroidal neovascularization
3-D	Three Dimensional
NDPR	Non Proliferative Diabetic Retinopathy
NN	Neural Network
MA	Microaneurysms
ML	Machine Learning
GLCM	Gray Level Co-occurrence Matrix
SVM	Support Vector Machine
MCC	Mathews Correlation Coefficient
PVV	Positive Prediction Value
TN	True Negative
TP	True Positive
FP	False Positive

FN	False Negative

NOMENCLATURE

$p(i, j)$	Intensity Probability of ith Row and jth Coulomb of Image
$(i - \mu_i)$	Pixel Intensity of ith Row is Subtract the Mean Pixel Intensity of ith Row
σ_i, σ_j	Intensity Variance Of ith Row and jth Coulomb
w^t	Weight at t-th Iteration
$\alpha_i, \alpha_j, y_i, y_j$	Coefficient of Lagrange of ith Row and jth Coulomb

SYNOPSIS

Macular edema is an advance stage of diabetic retinopathy which affects central vision of diabetes patients. The main cause of edema is the appearance of exudates near or on macular region in human retina. If the exudates are present in the macular region of retina, it will lead to diabetic macular edema. Early detection of macular edema in diabetic patients paves a path for prevention from blindness. The automatic system for early detection of diabetic macular edema should identify all possible exudates present on the surface of retina. In the proposed work, a computer added diagnosis system is design for the identification of the exudates in color retinal fundus images. The system consists of three stages; candidate exudates detection, feature extraction and classification. The system is designed with (i) background estimation, morphological reconstruction, normalization for candidate exudates detection (ii) Gray level co-occurrence matrix for feature extraction and (iii) support vector machine for classification. The classifier classifies in between the region of exudates and non-exudates. The system performance is evaluated in terms of the parameters such as sensitivity, specificity, mathews correlation coefficient, positive predicative value, and accuracy whose values are 88.23%, 100%, 88.23%, 100%, 93.75% respectively.

Keywords: Macular edema, Diabetic retinopathy, Exudate, Retina fundus images, Morphological reconstruction, Normalization, Candidate exudates detection.

CHAPTER1

INTRODUCTION

1.1GENERAL

The retina is a coated form of tissues. The designing of eye is like that, its capable to converting of incoming light into neural signal for further processing into the brain, which is the visual cortex. It is the tissue which is coating interior part of the eye. The function of retina to connected to the outside of the world. Retina makes with active tissue and highly metabolically and having a double blood supply. Thus, because of complicated architecture of the retina : The dieses of eye and brain due to the retina and some ocular dieses like glaucoma, macular degeneration, third and first most important causes of blindness in world, and diabetic retinopathy from diabetes second most common causes of blindness in the world. Retina is thin transparent tissue contain the number of layer in the back side of the eye.

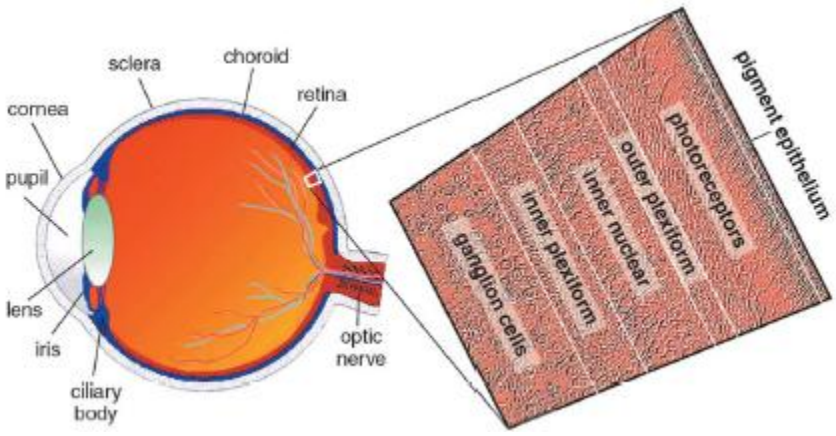

Figure1.1: cross-section view of eye and its major component

2-D and 3-D retinal imaging method, which is using in retinal fundus image and OCT images analysis. This imaging method is description of morphological operation and function.

This method using to improved the retinal disease diagnosis and image based system. The method which is development the efficiency for screen iterated computer aided detection of retinal dieses as well as clinical application.

1.2 EYE ANATOMY

The transparent cornea colored iris, opening the iris, black pupil, and white sclera is the visible parts of the eye. The partially image is focused, when rays of light coming from the cornea. Because light focus on the retina, its passing through the anterior chamber, the pupil, lens these all are spotting the image and goes to the vitreous.

The system of blood supply of the retina is based on two ways, primary form choroid and secondary from retinal vasculature which on the upper portion of the retina.

For useful application of the biological connectivity of retina and choroid are through the following layers, which are shows in below.

1) Internal limiting membrane
2) Nerve fiber layer
3) Ganglion cell layer
4) Inner plexiform layer
5) Inner nuclear layer
6) Outer plexiform layer
7) Outer nuclear layer
8) External limiting membrane
9) Pigment epithelium layer
10) Bruch's membrane

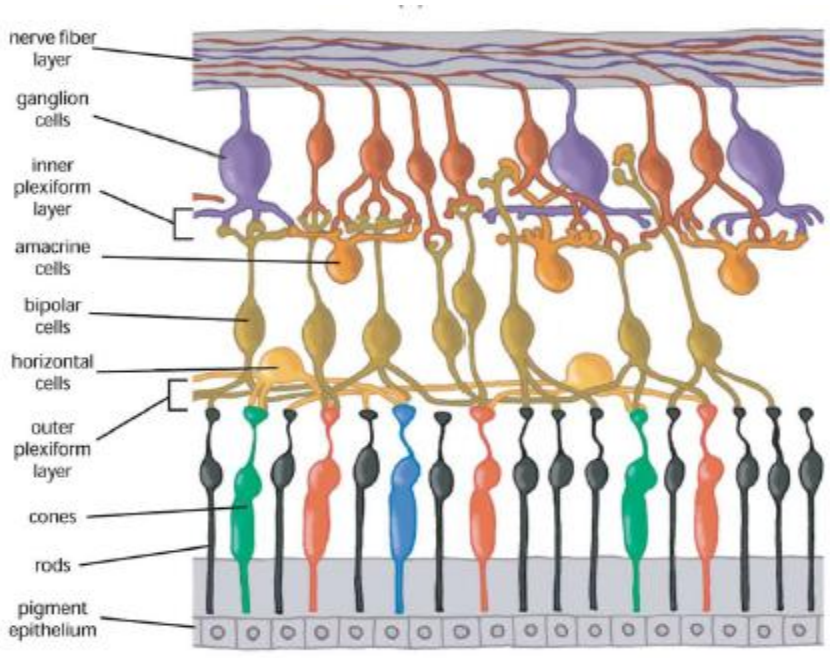

Figure1.2: Schematic drawing of cellular layer of retina

1.3 RETINAL SYMPTON OF EYE AND SYSTEMIC DISEASE:

There are many dieses, which originate either in eye, brain, or the cardiovascular system, but disease marked in the retina. These all disease via eye imaging and image processing analysis methods.

A) DIABETES:

The patient has fasting plasma glucose over 7.0 mm/l. The diabetic mellitus has been diagnosed. This definition has been organized by World Health Organization. Its causes are not fully understandable obesity, sedentary life style, and genetic background; all confer increased risk of developing diabetes. The following reason that increasing the risk of development diabetes, the medical treatment primarily through the insulin diet change and anti-hyperglycemic drugs due to hyperglycemic increase the blood glucose, damage the small and large blood vessel, also damage nerve cell. Later its effect damage kidney, brain, heart and eye. Due to this difficulty of diabetes is medically known as diabetic retinopathy.

B) DIABETIC RETINOPATHY:

Diabetic retinopathy (DR) is a problem of mellitus and second most common causes of blindness and visual loss. There is plentiful confirmation that yearly screening and early diagnosis blindness and visual loss can be prohibited. In the eye hyperglycemic expenses the wall of retinal vessel, due to this lead to

1) Ischemia, enlargement the new blood vessel. That bleeds reason of retinal aloofness. This process is called proliferative diabetic retinopathy. The fluid collection at the center of macula which is within or below the retina that causes visual dysfunction.

2) Blood-retinal barrier breakdown, leading the fluid leakage is called diabetic macular edema (DME) and that damage to photoreceptors. DME is type 2 diabetic and this is primary causes of visual loss with diabetes. There is intracellular and extracellular retinal tissue. Due to blood retinal barrier breakdown causes leakage of dilated hyperpermeable capillaries and microaneursyms. Clinically significant macular edema (CSME), if the area within 500m of the center (macula), due to DME the thickening of retinal relating to the center of the retina (macula). Definition of hard exudates is when at or within 500m from center with thickening of adjustment retina. Another definition is, if area of retinal thickening one optical disc area or larger in size, or any part of distance within one disc diameter of the center of the retina. This definition of CSME generally refers to the threshold level at which laser photocoagulation treatment is considered. While visual loss occurs when macular edema involves the visual center, lesser degrees of DME may cause visual deterioration.

C) EGE RELATED MACULAR DEGENARATION:

Age-related macular degeneration (AMD) is one of the common causes of visual loss in present ally emergent public health problem. The expectation of occurrence of AMD is double in next 25 years. There are two main type of AMD, 1) Dry AMD this gradually loss the visual sharpness. 2) Wet AMD another name is called chorodal neovasularization (CNV), this is characterized by growth of a chorodal vascular structure into the macular accompanied due to increasing vascular permeability. The increasing of dry AMD can be control or slowed in many patient through some dietary medicine supplements, but in the case of wet AMD is treated with intravitreal

administration of anti-vascular growth factor. the most common cause of visual loss and is a emergent public health problem.

D) GLAUCOMA:

Glaucoma is the third most principal reason of blindness, due to damage of optical nerve reason of visual loss field. Early treatment are minimized the visual damage. Glaucoma is not retinopathy is primarily neuropathy. Glaucoma occurs in retina due to damaging of ganglion cell and also there axons. cause of blindness, characterized by steady damage to the optic nerve and resultant visual field loss. Early diagnosis and best possible treatment have been shown to minimize the risk of visual loss due to glaucoma. Basically glaucoma is primarily a neuropathy, not a retinopathy, and acts on the retina by damaging ganglion cells and their axons. The trademark of glaucoma is drawing blood from the surface of the person by forming a partial vacuum over the spot of the optical disc, which show the optical nerve head 3D structure. The method of optic disc can be imaged two-dimensionally either through indirect stereo color fundus photography or indirect stereo biomicroscopy. The cup to disc ratio, is important structure indicate for detecting the presence and progress of glaucoma.

Diabetic retinopathy (DR) is a progressive eye disease that currently affects millions of people worldwide. Diabetic macular edema (DME) is a complication of diabetic retinopathy and it is a common cause of vision impairment and blindness [1]. DME is one of the complications caused by diabetes; DME may lead to visual damages in people at a working age. However, the risk of vision loss and blindness may be reduced if DME is detected early, and followed by appropriate treatment. DME occurs from swelling of the retina in diabetic patients due to leaking of fluid from micro aneurysms within the macula. This presentence of fluid causes retina thickening in diabetic patients which is termed lipid deposits also known as exudates. Exudates appear as bright structures with well defined edges and variable shapes**.**

Study in medical imaging has shown that most of the exudates screen themselves in the human retina**.** This leads to a clear road for researchers to device and improve the method for analyzing exudates. Therefore, specialized image processing method is used to obtain proper identification of exudates in retinal fundus images [2-3]. These image processing methods may

help to medical professionals in timely diagnosis of DME and improve medical facilitation available to the patients**.**

1.4 TYPES OF DIABETIC MACULAR EDEMA

There are two types of macular edema, (i) Non Clinically Significant Macular Edema (Non-CSME) and (ii) Clinically Significant Macular Edema (CSME). Non-CSME is a mild form of edema in which there are no symptoms of the disease because the locations of exudates are at a distance from fovea and the central vision is not affected. CSME is the severe form of edema in which the exudates leak out and get deposited very close to or on fovea affecting central vision of the eye [4]. Fig.1.5. is an example of retinal fundus image showing digital image of human retina along with its main components and exudates.

1.5 METHOD OF DIAGNOSING MACULAR EDEMA

Many methods for diagnosing macular edema and other retinal diseases are discussed in literature [5-7]. Also exudates segmentation and classification method presented in the literature are based on: Thresholding and morphological methods, thresholding method analysis [8], Thresholding methods identify the exudates by local and global analysis of threshold whereas morphological methods first identify all the structure of predictable shape and removed them afterwards for easy detection of exudates in retinal fundus images [9-12]. Also, there are number of classification method to classify various lesion types in retinal images such as drusen, cottonwood spot, exudates [13-14]. In this work classification is performed in between exudates and non-exudates region on pixel to pixel basis, which will further aid to ophthalmologist in diagnosis of patient diabetic macular edema.

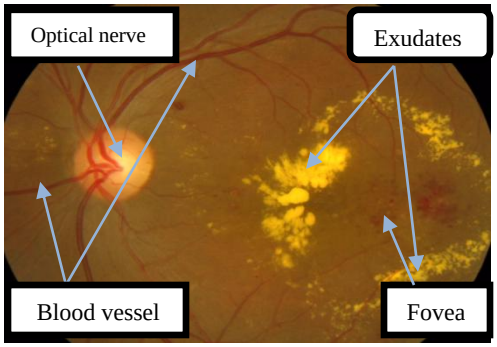

Figure1.1: Digital fundus image of human retinal along with its main components and exudates

CHAPTER2

LITERATURE REVIEW

The previous research works to identify exudates on retinal fundus images are based on two main criteria. 1) Lesion based 2) image based. These two method are exudates detection technique assessing the accuracy of the method. In lesion based criteria segmented of exudates region in abnormal retinal image using the appropriate segmentation technique. The lesion base accuracy can be measured in terms of region sensitivity and specificity. The method of finding lesion-based accuracy can be either a pixel level basis or alternatively using large collection of pixel eg,: 10x10, 20x20 slice. Phillip et al [15,16] has investigation the exudates detection and identification. The contrast of the exudates are enhanced, then further Thresholding method are using nether global or local. Which are segment exudates lesion, the sensitivity report between 61% and 100% . This technique is based on 14 images.

Singer et al. [1] determine the appropriate patient, method, and timing for screening for diabetic retinopathy. The screening of retinopathy is justifiable if early detection leads to less vision loss at an acceptable cost. The evidence show that 1) laser therapy reduce the rate of vision loss by 50% among patient with proliferative retinopathy and macular edema; 2) duration of diabetic is the main risk factor for retinopathy; and 3) standard ophthalmoscopic examination has only moderate sensitivity about 80% and specificity greater than 90% for proliferative. Estimates of cost effectiveness indicate that screening for retinopathy not only save year of vision but may be cost saving from a collective perspective.

Abramoff et al. [2] says that fundus camera is creation of automatic screening system which promptly able to detection of diabetic retinopathy. The image quality judging is automatically approach based on some documented. We proposed a new set of feature. The initial result estimate image quality.

Philip et al. [3], says that diabetic retinopathy screening program Anonymised images were obtained from consecutive patients, in automatic grading algorithms a training set of 1067 images was used. Separate test of 14406 images from 6722 patient was tested during final

software. Parameter like sensitivity and specificity in terms of manual and automatic operation as disease/ no disease grade were determined relative to a clinical reference standard.

Abramoff et al. [4] says that, important eye diseases manifest themselves in the retina, this review is focused on the analysis of the retinal image. Today industrial world most causes of occurrence blindness is age related macular degeneration, glaucoma and diabetic retinopathy. This review is devoted to analysis method of retinal image and their clinical approach. Method for 2-D fundus images and 3-D optical coherent tomography images are reviewed. The quantitative technique for analysis of fundus photographs with a focus on clinically related evaluation of retinal vasculature, identification of retinal lesion.

Akram et al. [5], proposed a digital diabetic retinopathy system for early detection of diabetic retinopathy. NDPR consists of both dark and bright region but it consists of blood vessel and optical disc, difficult to classify. So it's segment them out prior to lesion detection. Preprocessing is the first step to separate the background area from the noise image. It's enhanced the quality of retinal image and also minor the processing time. After preprocessing blood vessel enhancement, using the gabor wavelets and multi layer Thresholding respectively. Then find out the location of optical disc using average filter and Thresholding. Optical disc boundary detection using Hough Transform and edge detection. Dark and bright lesion detection using hybrid fuzzy classifier. The proposed system gives comparable result and can be used in a computer added system for early detection of diabetic retinopathy.

Ege et al. [17] proposed work on the location of exudates and cotton wool tested on 38 color images. The initial detection is using a combination of templates masking, region growing and thresholding technique. Bayesian classifier based technique was classified the bright region into cotton wool spots, exudates and noise. The performance of classification was 62% for exudates and 52% for cotton wool spots.

Wang et al. [18] detecting some good result, this technique achieved 100% sensitivity and 70% specificity. Bright region lesion detection such as cotton wool and exudates are based on minimum-distance discrimination. The NN network has classify the retinal exudates. Hunter

et al also using the same technique for classification. The NN was trained to discriminate exudates from drusen based of 16x16 pixel scale.

Walter et al. [12] green channel of retinal images is used for identification of exudates. After initial localization, mathematical morphological technique is determined the exudates. This method has three parameter 1) size of local window 2) two other thresholding. The minimum variation within each localization is determined the first threshlding value. The candidate exudates region based on first thresholding value. The surrounding background pixel change in the second thresholding to be classify the exudates. This technique was achieved 92.8% sensitivity and 92.8%. predictivity asset of 15 abnormal retinal images.

Niemeijer et al. [19] distinguished the bright lesion, i.e., exudates, cotton wool spot, and drusen from color retinal images. The lesion probability map is the first step of image pixel classification characteristic. Each probable cluster was assigned the likelihood that the cluster was a true bright lesion. these clusters were classified as exudate, cotton, wool spot, or drusen.

Goldbaum et al. [20] have discriminated similarly colored objects in retinal images based on color information, not many work have shown interest in color classification of retinal images.

Alireza et al. [21] proposed a method base on computational intelligent technique for automatic segmentation of exudates region. Segmentation method using fuzzy c means clustering follows some preprocessing steps. In color retinal image some set of initial feature are extracted like color, size, edge strength and texture for classification. This classification is classify the exudates and non-exudates region.

Ahmed et al. [22] proposed a method to automatically segment optic nerve and exudates. In the algorithms, they used preprocessing steps such as averaging filter, contrast adjustment, Thresholding, morphological opening, watershed transformation on the green component of the image. This method yielded sensitivity 96.7%.

Chugh et al. [23] detection of exudates such as uses homogeneity of healthy areas rather than unhealthy areas. In this method first extracted the healthy area such as optical nerve using sobel filter method and blood vessel by entropy thresholding method. Thresholding method is segmented exudates from diabetic retinopathy images. The proposed method yields accuracy 90%.

Fleming et al. [29] Automatic grading of the image by health boards so that human grading task is reduced. Microaneurysms (MAs) are the earliest sign of disease for classifying whether images show the retinopathy. In this paper describe automatic method for MA detection and image contrast normalization can improved the ability to distinguish between MA and other dots that occur on the retina. method of contrast normalization is watershed transform, that result not contain no vessel or other lesion. The image containing MAs detecting with sensitivity 85.4% and specificity 83.1%.

Kirsch et al [33], The class of algorithms is describe which enables computer quantized images to be decomposed into constituent reflecting the structure of the images. This decomposition is viewed as the morphological precursor to a highest level syntactic analysis. Numerical result of typical biological are presented.

Kohavi et al. [35] proposed a machine learning (ML) which is reliable tool in medical domain researcher. For medical decision support newly technique medical imaging. This experiment is automatic learning method for this task and also for patient management healthcare. For more efficiency medical care the ML is tool, which computer based system can be participation in the health care field. This paper is description of a ML based methodology for identification health care improvement. In the medical paper, the extract the view of disease and treatment and bridge the reaction between disease and treatments.

CHAPTER 3

MATERIALS AND METHOD

3.1 MATERIALS:

MESSIDOR, a publicly available dataset is used to test performance of segmentation and classification for exudation. The MESSIDOR[24] dataset containing 80 fundus images with exudates region with Zeiss Visucam PRO fundus camera, at resolution of 1449x2201 pixel and with a 45° Field of view. The image capturing process is vetted by automatic quality assessment algorithms based on the Elliptical local vasculature density feature [25-26].

3.2 METHOD

Computer aided diagnostic system is a process for identification of exudates in retinal fundus image is present, which will further help. Exudate as a bright region as a bright spot and patches in fundus image. Obviously it's a high contrast ever in other component in the fundus image. Automatic system is smoothing the dark region and enhanced the contrast of bright region [27]. In this work, morphological reconstruction is used to smooth dark region such as haemorrhages and blood vessels [28]. For easy lesion detection, contrast enhancement is improved the contrast of the object. Image normalization technique used for detection all possible bright regions [29]. Texture representation and discrimination is after the image normalization approach. The binary candidate region for exudates was extracted by applying a low adaptive Thresholding value [30]. The region was segmented by the thresholding, enhanced image also contain optical nerve region and pixel due to their similarity with exudates. For correct detection the false and unauthentic pixel should removed before the classification stage. The proposed system segmented optical nerve using masking of related area where optical nerve probability in fundus image data base system.

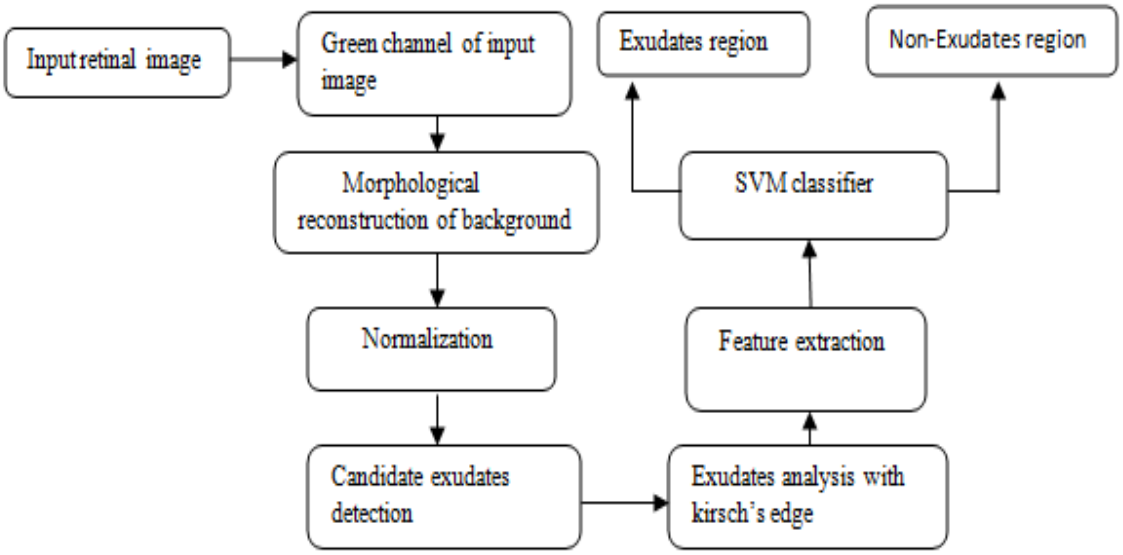

Figure3.1: Proposed computer added diagnosis system for the identification of exudates in retinal fundus image

I) SELECTION

The green channel is selected because of better contrast of this channel then the rest two channels and it will further help in extracting brightest region from background.

II) PREPROCESSING

Selected green channel of retinal fundus images are passed through the various preprocessing steps in order to detect the region of exudates. The first step is the application of a big size median filter shown in the work of Niemeijer et.al [31], showed that the size of the median filter should be $1/30^{th}$ of the height of the fundus image for background estimation. After that estimated back ground is subtracted from original image. The step has great computational performance advantage by avoiding the multiple passes.

III) IMAGE NORMALIZATION

Image normalization is the process where highest intensity of image is centered at zero. We enhanced the normalization with addition of morphological reconstruction [29]. It improved the nerve fiber layer and other structure of edges of optical nerve, without any expansion of exudates region. The histogram showed the clear division between dark structure and bright structure. The

dark structure like macula, vasculalature are located at the left side of the histogram. On other hand bright structure are formed on the positive side of the histogram. Which contain the optical nerve, bright lesion such as exudates and other structure related to very bright retinal pigment epithelium layer. Because of the alignment of the histogram after the normalization we can select all exudates candidate region.

The method of optical nerve removal [32], it is understandable that the similarity of potential of color between optical nerve and exudates in fundus image. The optical nerve detection is the mature technique. So we only concentrate to exudate detection. We did not implement automatic optical nerve detection in our paper. We did manual removal of optical nerve by the having size slightly greater than optical nerve.

IV) EXUDATES EDGE DETECTION

The exudate detection is performing by conveying a score for each exudates candidate. The exudate candidates are selected by running 8-neighbour connected component analysis of exudates candidate region. The way of implementation is based on Kirsch's Edges [33]. The advantage of this method is the edge value of inner and outer part is higher in the exudates region as compare to non-exudates region. Kirsch's edges is based on kernel k to evaluate at 8 different direction and capture the external edge of the lesion candidate. When the kernel output compare together for the maximum value found on each pixel output.

It computes the gradient by convolution the image with eight template impulse response arrays as shown in figure. The scalar factor is 1/15.

$$K= \begin{matrix} \frac{5}{15} & \frac{-3}{15} & \frac{-3}{15} \\ \frac{5}{15} & \mathbf{O} & \frac{-3}{15} \\ \frac{5}{15} & \frac{-3}{15} & \frac{-3}{15} \end{matrix} \qquad (3.1)$$

Convolving the image with eight impulse response array are method of finding the gradient of different direction. The largest gradient among different direction is to be set as final gradient. This kirsch's method is enhanced the edge. Pixel belonging to the edge or not is determine by the Thresholding, which are set after the edge enhancement.

Thresholding based technique focus on a global or adaptive gray level analysis, but the automatic selection of proper Thresholding is difficult due to uneven illumination of the image.

V) FEATURE EXTRACTION

Simplification of larger set of data accurately in amount of resource are available is called feature extraction for classification algorithms. Large number of variable required large memory and computational power. For image analysis and pattern reorganization texture players significant role. In this proposed method statistics texture feature obtained is formulated texture feature have using in real time pattern recognization application due to high discrimination lesion accuracy. In this proposed method, Gray level co-occurrence matrix (GLCM) is formulated to obtain statistical texture features. There are two types of texture feature measures. They are first order and second order measures. GLCM is the second order texture calculation. In second order texture measures consider relationship between neighbors. But first order texture measures are statics, consider not pixel neighbor relation. Texture features have high discrimination accuracy, requires less computation time and hence efficiently used for real time Pattern recognition applications.

A) GRAY-LEVEL CO-OCCURRENCE MATRIX CONSTRUCTION:

A GLCM is a square matrix which have equal the no of row and columns to gray level in the image, which having certain properties about the spatial distribution of the gray levels in the image texture. Actually this matrix gives the spatial relations with to a neighboring pixel value. Where pixel value i reference pixel is relation with neighboring pixel j, so each element (i,j) of the matrix represent the number of occurrence of the pair of pixel with pixel value i and j which are a relation distance d from each other. There are much method specifying the spatial relation between two neighboring pixel with different offsets and angles, the default one being between a pixel and its immediate neighbor to the right, mainally four possible spatial relationships (00, 450, 900 and 1350) are specified and implemented.

Mathematically, the elements of a G×G gray-level co-occurrence matrix MCO with displacement vector **d**(=dx, dy), for a given image I of size N×N is defined as:

$$M_{CO} = \sum_{x=1}^{N} \sum_{y=1}^{N} \begin{cases} 1, if I(x,y) = i and I(X + d_x, y + d_y) = j \\ 0, otherwise \end{cases} \quad (3.2)$$

Figure 3.2: describes how to compute the GLCM. It shows an image and its corresponding co-occurrence matrix using the default pixels spatial relation, offset = +1 in x direction. Each element of the GLCM is the number of times that two pixel with gray tone i and j are in neighborhood at the distance d and direction θ.

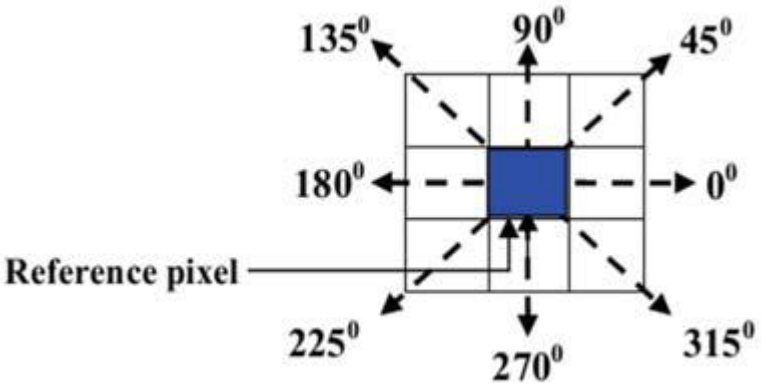

Figure3.2: Co-occurrence matrix direction for extracting texture feature

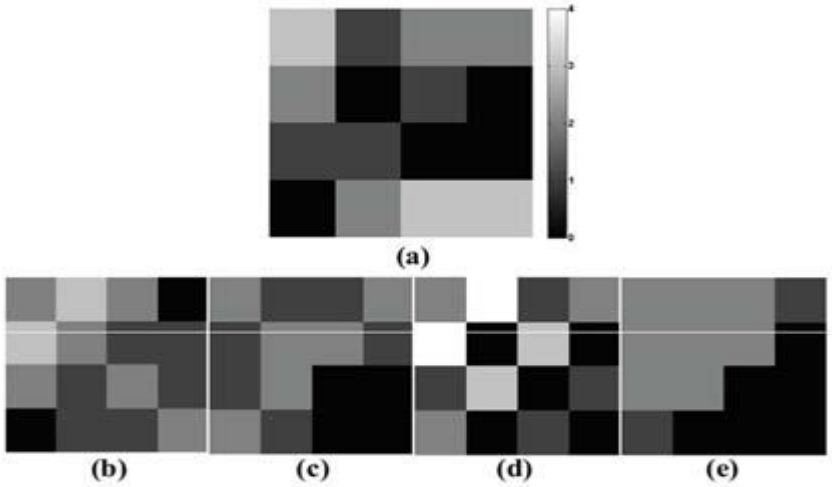

Figure3.3: GLCM construction on a (a) test image along four possible direction (b) 0^0 (c) 45^0 (d) 90^0 and (e) 135^0 with a distance d =1

B) DIRECTION AND OFFSET:

Parameter 'd' ranges starting from 1 to size of the image and θ is the angle of four discrete directions (0°, 45°, 90° and 135°). Using the large value of d (d >2) values to a fine texture would result in a GLCM matrix that does not give a detailed textural information. By simulation it was found that, construction of the GLCM with d=1.Its shows better results than that with d=2. This can be explained by the fact that it is more likely for a pixel to be correlated to a closely located pixel than to one located far away. Therefore, we have presented the results for d = 1 only. Direction 'θ' is another important parameter which gives different textural properties along different directions. This is evident from Fig.3.3 where the GLCM matrix along different angles is distinctly different from each other. Every pixel has eight neighboring pixels allowing eight choices for θ, which are 0°, 45°, 90°, 135°, 180°, 225°, 270° or 315°. Fortunately, as these matrices are symmetric, it is more convenient to use the upper or lower diagonal matrix coefficients in forming the vectors. Hence, the co-occurring pairs obtained by choosing θ equal to 0° would be similar to those obtained by choosing θ equal to 180°. This concept extends to 45°, 90° and 135° as well. Hence, one has four choices to select the value of θ. Sometimes, when the image is isotropic, or directional information is not required, one can obtain isotropic GLCM by integration over all angles.

GLCM is defined the distribution of co-occurrence values over an image at given off-set in GLCM matrix, the number of gray level is equal to number of row and colums. In image processing literature the early proposed method is use the statistical feature. Haralic [34] suggested the use of co-occurrence matrix of GLCM. The feature extraction from GLCM is Energy, Contrast, Entropy, Correlation and Homogeneity.

1. Contrast- it is a measurement of intensity contrast between a pixel and its neighborhood pixels in the whole image.

$$\textbf{Contrast} = \sum_{i,j} |i - j|^2 \, p(i, j) \qquad (3.3)$$

2. Correlation – It is a measure of how a pixel is correlated to its neighborhood pixel in whole image.

$$\textbf{Correlation}=\sum_{i,j}\frac{((i-\mu_i)(j-\mu_j)\,p(i-j))}{\sigma_i\sigma_j} \quad (3.4)$$

3. Energy – It is the sum of squared elements in GLCM. It ranges from 0 to 1. For constant image, energy value is 1.

$$\textbf{Energy} = \sum_{i,j} p(i,j)^2 \quad (3.5)$$

4. Homogeneity – The closeness measurement of the elements distribution in GLCM to GLCM diagonal.
5. $$\textbf{Homogeneity} = \sum_{i,j}\frac{p(i,j)}{1+|i,j|} \quad (3.6)$$

VI) CLASSIFICATION

Classification based technique supervised approaches attempt to extract different feature and then use a classifier to classify the exudates and non-exudates region. Support vector machine (SVM) classifier is used to classify the Exudates and Non-Exudates regions.

A) SVM CLASSIFIER

SVM is learning algorithms using for classification and regressive analysis. That analyzes data and recognize pattern. It's basically a supervised learning model. The basic SVM takes a set of input data and predicts, for each given input. The working process of SVM is divided data into training, testing phase. The known data is training phase and data to given is testing is unknown. Accuracy of the classification depends on the efficiency of the classification. Variety of pattern reorganization problem SVM classifier has real excellent performance over there.

High dimension feature space in SVM and input space is mapped. The separation between the classes hyper plane is maximized the margin. Support vector is a point lie closest to the detection surface and directally affect the location. Optimal hyper plane is minimized the probability of classification error. When the classes are non separable, and the optimal hyper

plane is general method of construction which separate from data belonging to two different classes linearly separation is as follows.

$w^t x+b=0$ the hyper plane which satisfies the following condition

$$y_i(w^t x_{i+b}) \geq 1,\ i=1,2,\ldots n \qquad (3.7)$$

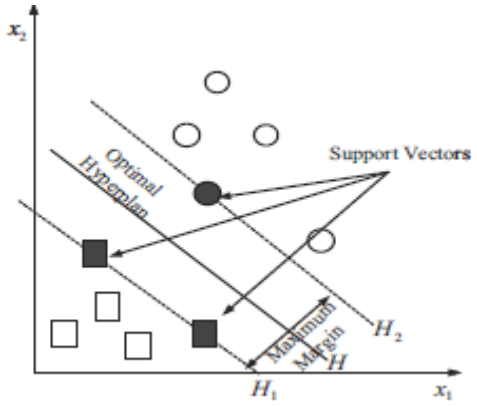

Figure3.4: optimal Hyper plan, maximizing margin and support vectors

Hyper plane optimal amount of maximization the margin $\frac{2}{\| w \|}$ that hyper plane is equivalent to minimized $\frac{\| w \|^2}{2}$ under the constrain(3.7) with have optimal maximizing the margin $\frac{2}{\| w \|}$. The linear constrain is problem when given below minimization of quadratic objective function larger principle are applying for quadratic problem of dimension (m) according to

$$\min \frac{1}{2} \| w \|^2 \quad \forall i, \alpha_i, y_i (w^t x_i + b) \geq 1 \text{y} \qquad (3.8)$$

By applying the principle of Lagrange, one obtains the quadratic problem of programming of dimension m (a number of examples) according to

$$\max \sum_{i=1}^{n} \alpha_i - \frac{1}{2} \sum_{i,j=1}^{n} \alpha_i \alpha_j y_i y_j (x_i x_j) \forall i, \alpha_i \geq 0 \qquad (3.9)$$

$$\sum_{i=1}^{n} \alpha_i y_i, i = 1,2..., n \qquad (3.10)$$

The coefficient of lagrange(α_i)

The solution for the optimum boundary $w^{\bullet}$ is a linear combination of the subset of the training data, the support vectors. The support vectors define the margin edges.

The function of classification class(X) is defined by:

Class(X) is lower than 0, X is in the the class -1, if not it is in the class 1.

The SVM were conceived primarily for the problems with 2 classes, however several approaches making it possible to extend this algorithm to the cases N classes were proposed. Generalization in the case multi-classes can be done in three different ways, they are one-against-one SVM, one-against-all SVM and global method.

To test the robustness of the SVM multi-classes in the case of automated detection of diabetic retinopathy, we used the approaches: one-against-all.

In both cases, a Gaussian core was used for discrimination with a bandwidth . The parameter of penalization C was fixed at a sufficiently high value so that the error of training remains weak (C=1000).

VII) PERFORMANCE MEASURMENT AND PERFORMANCE EVALUTION:

Confusion matrix [35] is measurement of used to performance evolution of the system. The measurer parameter is Sensitivity, Specificity, Accuracy, Mathew correlation coefficient Different measures are used to evaluate the performance of the system. The measures used are Accuracy, Mathews correlation coefficient (MCC), Sensitivity, Specificity and Positive prediction value (PPV). Confusion matrix evolution performance of such system using data in matrix which are commonly evaluate and its contain information about classification done by classifier about actual and predicted.

Table1

Confusion Matrix

		Predicted	
		Negative	Positive
Actual	Negative	TN	FN
	Positive	FP	TP

TN (True negative) – Prediction is correct as normal

FN (False negative) – Prediction is incorrect as normal

FP (False positive) – Prediction is incorrect as abnormal

TP (True positive) –Prediction is correct as abnormal

The accuracy is the percentage of prediction that is correct

$$\text{Accuracy} = (TP + TN) \div (TP + FP + TN + FN) \quad (3.11)$$

The Matthews correlation coefficient is used in machine learning as a measure of the quality of binary classifications.

$$\text{MCC} = (TP \times TN - FP \times FN) \div (\sqrt{(TP + FP)(TP + FN)(TN + FP)(TN + FN)}) \quad (3.12)$$

The sensitivity is the percentage of positive level instances that were predicted as positive.

$$\text{Sensitivity} = (TP) \div (TP + FN) \quad (3.13)$$

The specificity is the percentage of negative labeled instance that were predicted as negative.

$$\text{Specificity} = (TN) \div (TN + FP) \quad (3.14)$$

The Positive Prediction Value or precision rate is the percentage of positive prediction is correct.

$$\text{PPV} = (TP) \div (TP + FP) \quad (3.15)$$

CHAPTER4

RESULTS AND DISCUSSION

I) GREEN CHANNEL SEPERATION

The abnormalities are more visible in the green channel. So separation of green channel from RGB images is needed. The separate green channel images is show in figure 3(a, b, c, d).

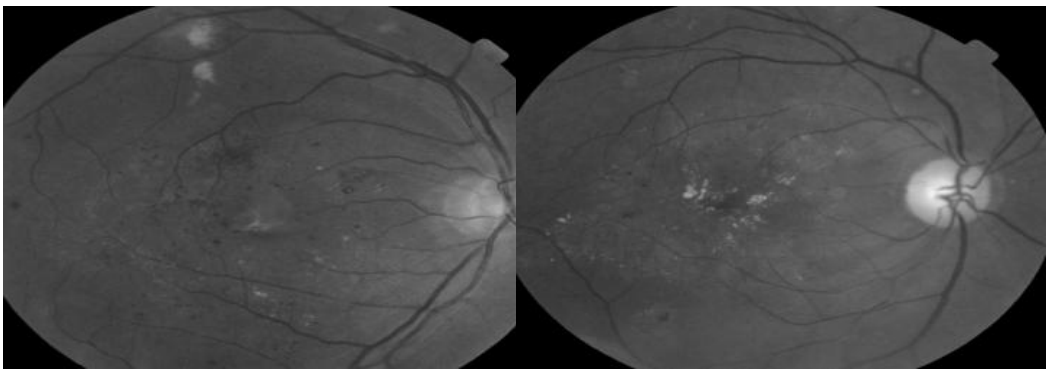

(a) (b)

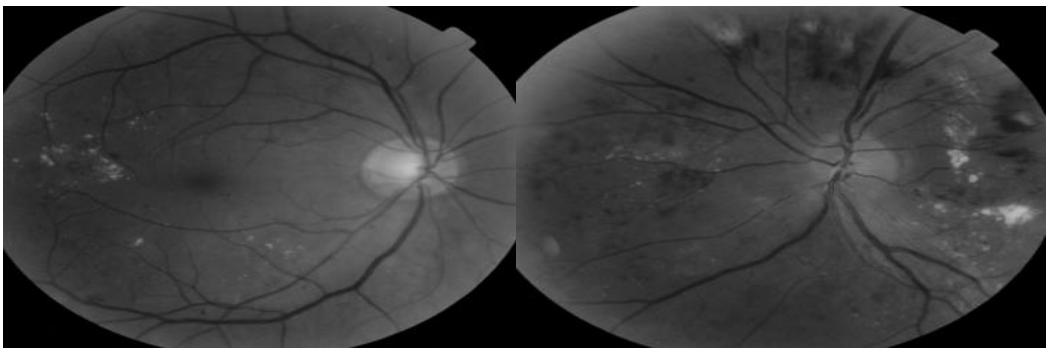

(c) (d)

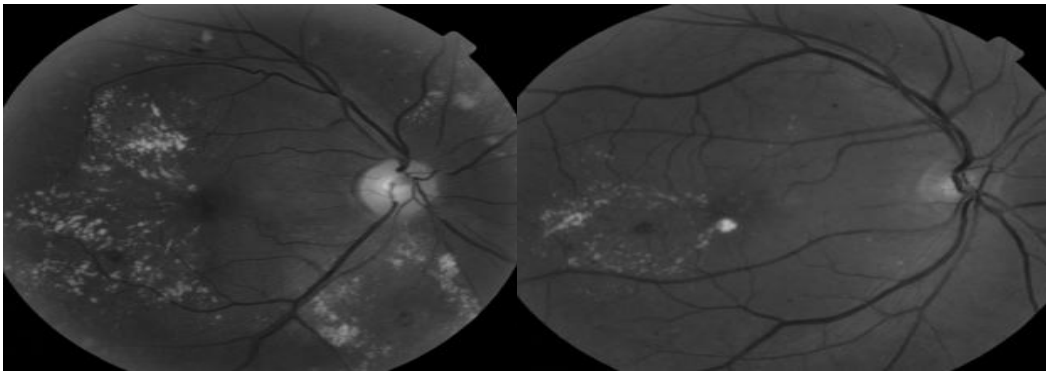

(e) (f)

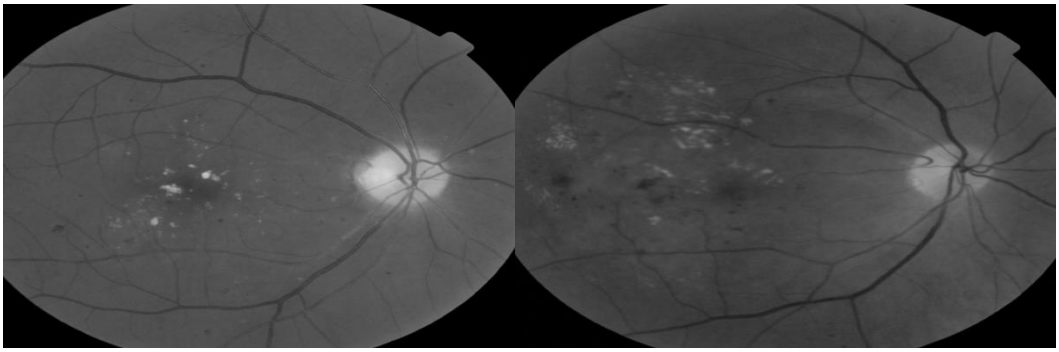

(g)

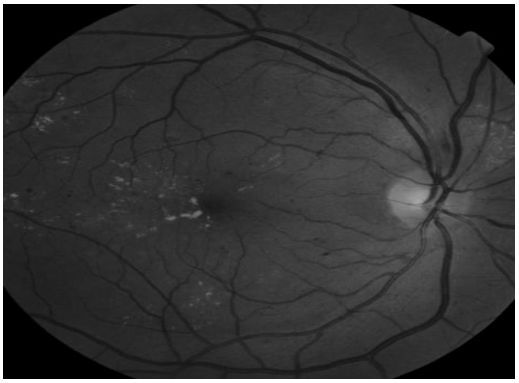

(h)

(i)

Figure4.1: a, b, c, d, e, f, g, h, i green channel of retinal fundus image.

II) MEDIAN FILTER AND BACKGROUND ESTIMATION

A) MEDIAN FILTER:

In the green channel, noise is present. Hence median filter is using. The median filter is best in removing salt & pepper and impulsive noise based on non-linear digital filter technique. Median filter is preserving sharp edge, erased black dots called pepper and fill in white holes in the image called salt. The method of working is median pixel value of intensity of neighborhood replaced at each pixel of the image matrix. As can be seen figure 4(a, b, c, d, e, f, g, h, i).Here using the big size window of median filter because saving the bright region of the image

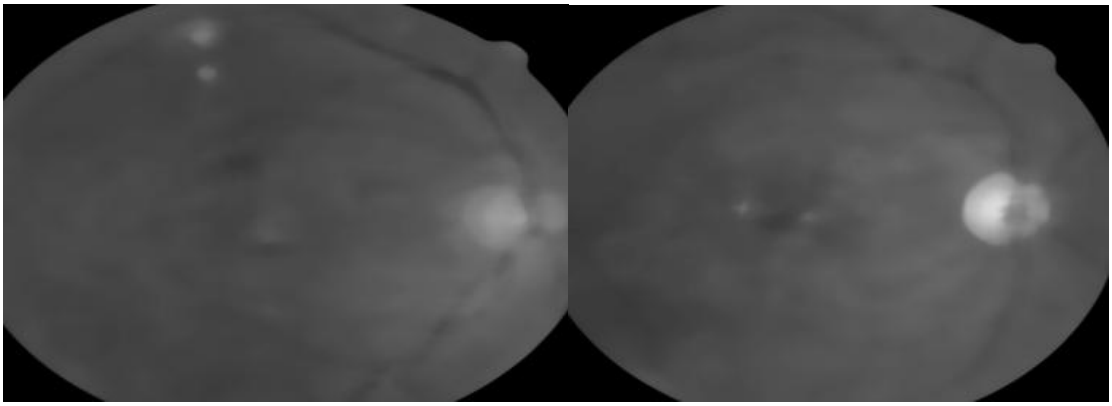

(a) (b)

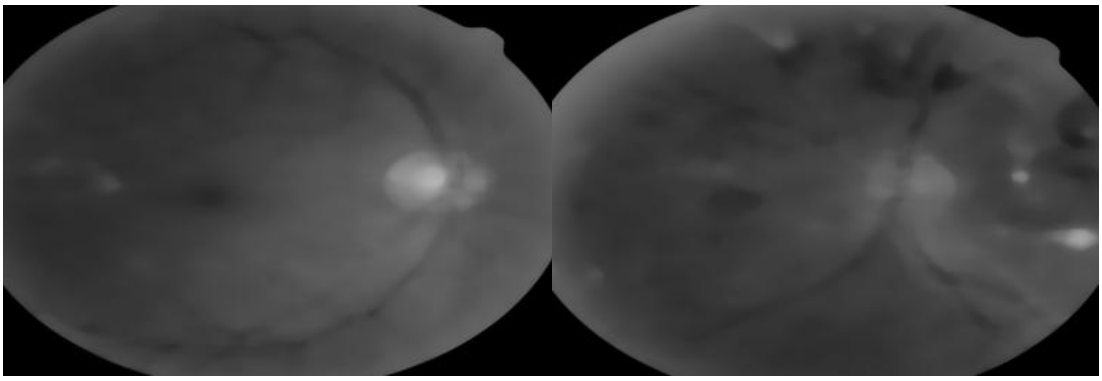

(c) (d)

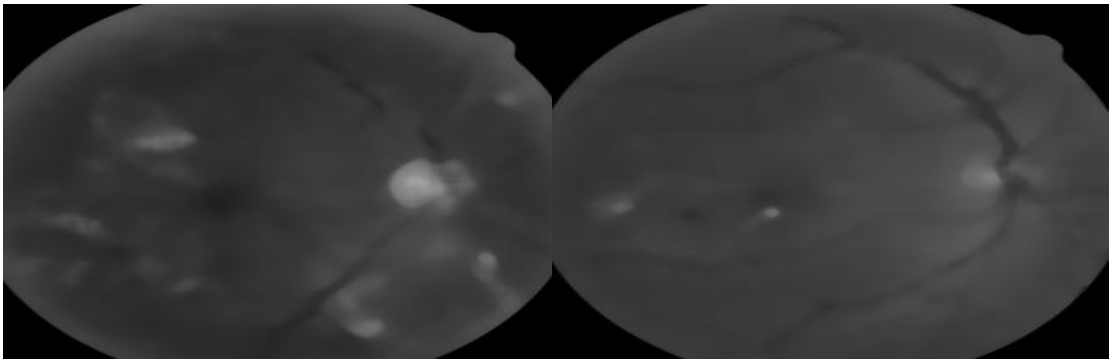

(e) (f)

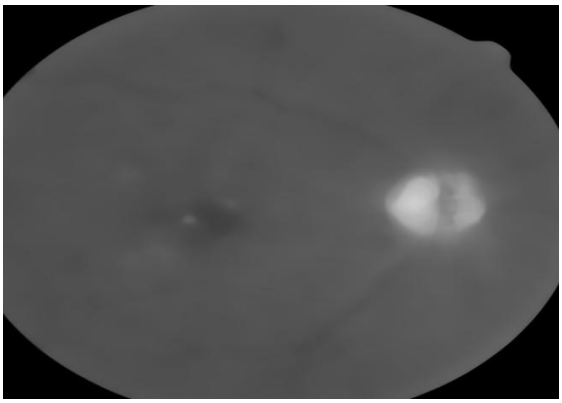

(g)

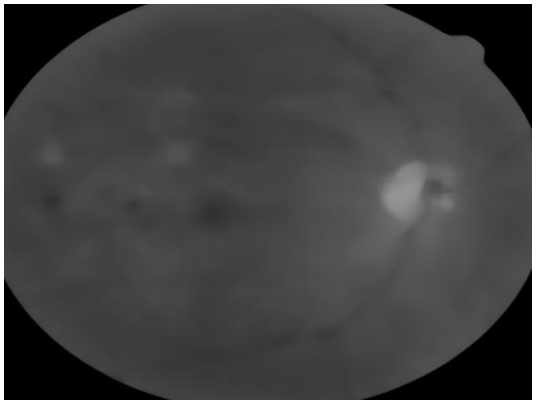

(h)

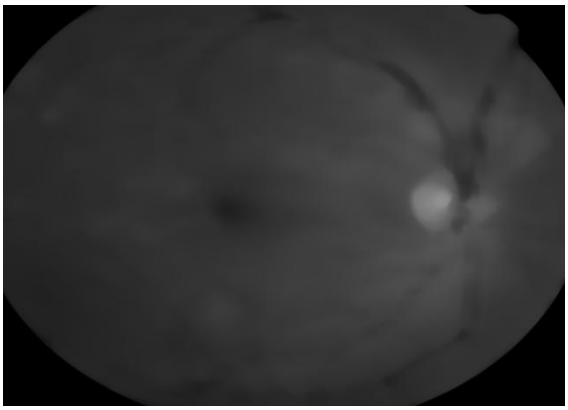

(i)

Figur4.2: a, b, c, d, e, f, g, h, i show retinal fundus image after applyinf median filter

B) BACKGROUND ESTIMATION:

Due to using median filter some bright region information are lost. For recovering of that information we are estimating the background. As shown in figure 5 (a, b, c, d). In retinal image database containing 1449x2201 pixel configurations, where 1449 rows are present there. So in result (49x49) size of median filter window, this result is good contrast between exudates and background. This approach has great computational performance advantage avoiding the multiple passes. After that estimated background is subtracted from the original image in order to obtain a normalized version, in proposed method, enhanced the normalization with morphological reconstruction

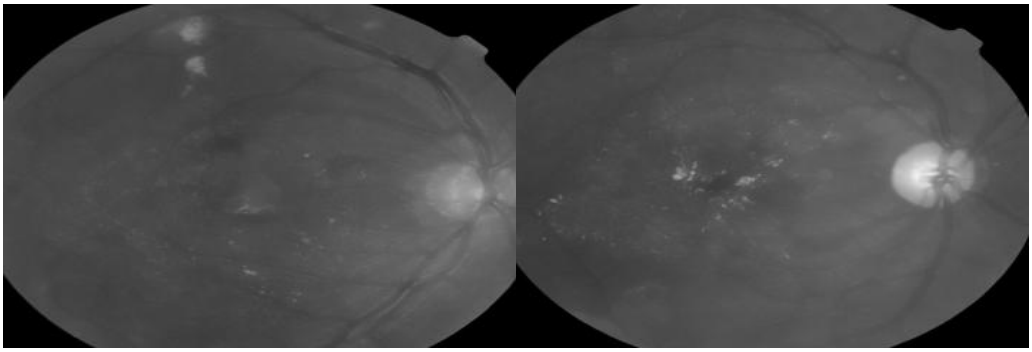

(a) (b)

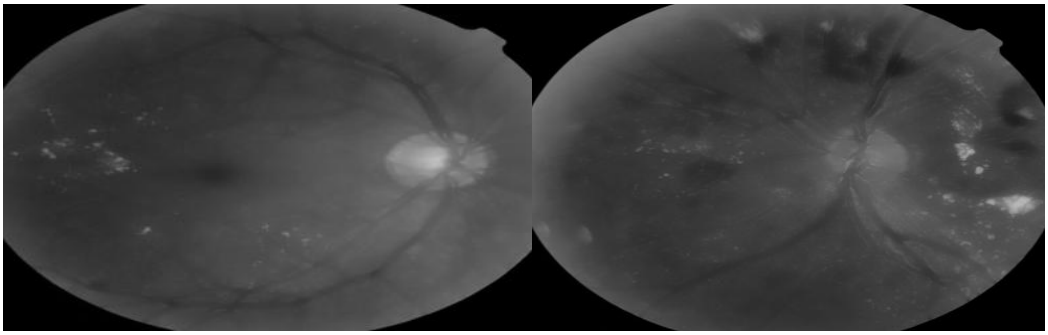

(c) (d)

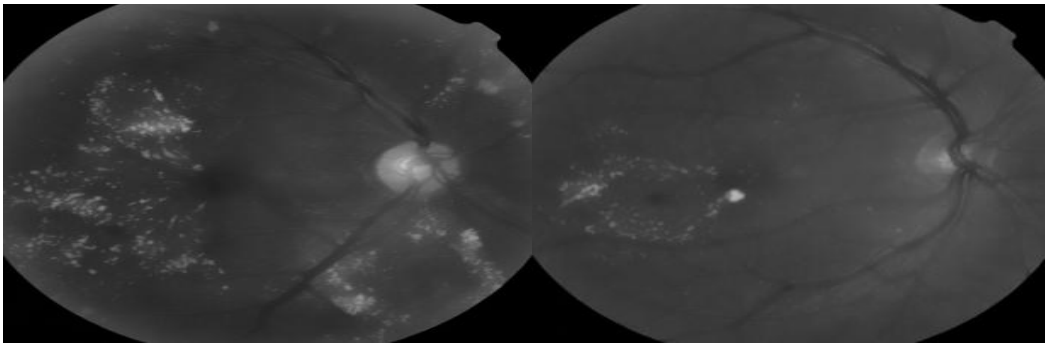

(e) (f)

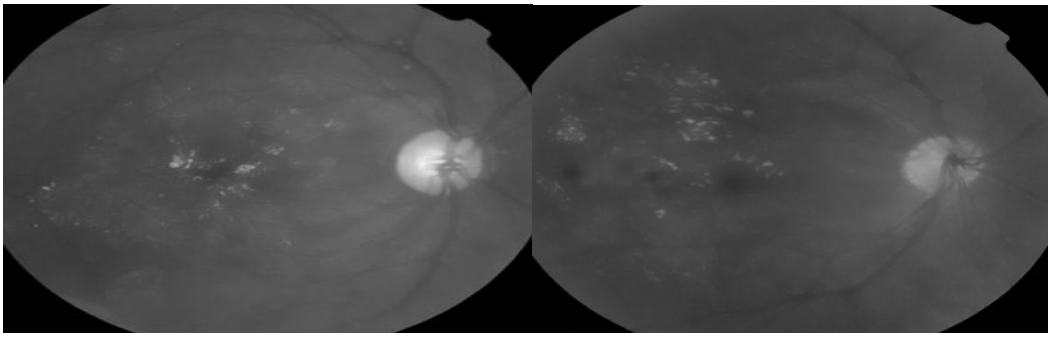

(g) (h)

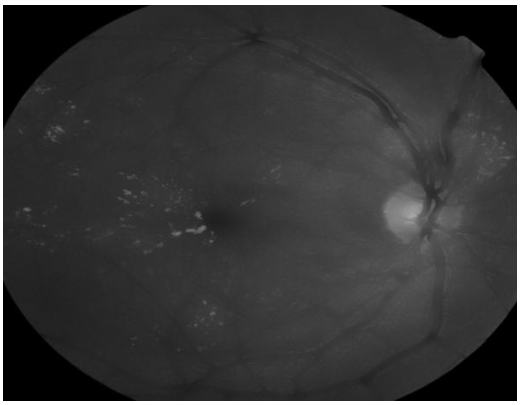

(i)

Figure4.3: a, b, c, d, e, f, g, h, i show the retinal fundus image after background estimation

III) MORPHOLOGICAL RECONSTRUCTION

In morphological reconstruction process one image called the marker, based on the character of another image, called masked. The high point and the peak in the marker image specify where processing begins. The peaks spared out or dilate while being forced to fit within the mask image. The scattering processing continues until the image value stop changing as shown in figure 6(a, b, c, d, e, f, g, h, i).

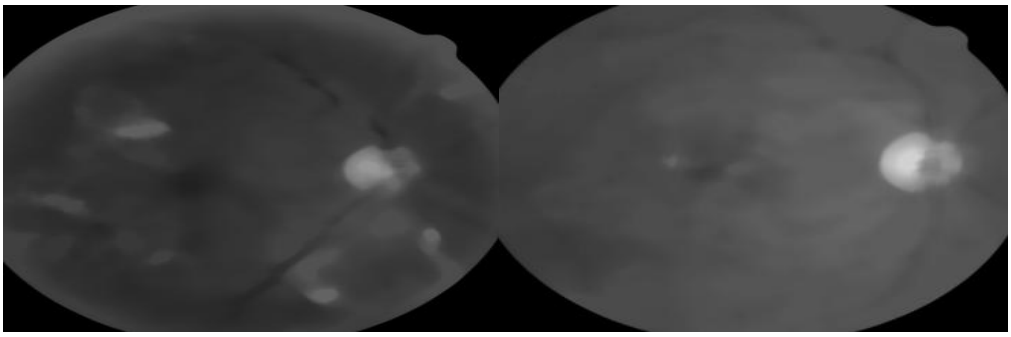

(a) (b)

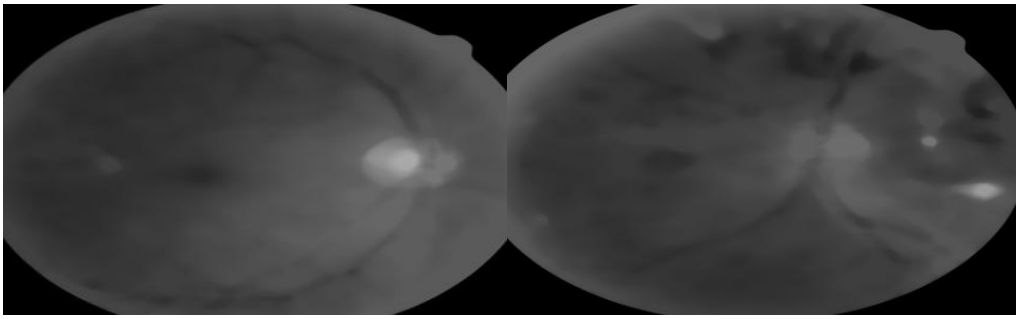

(c) (d)

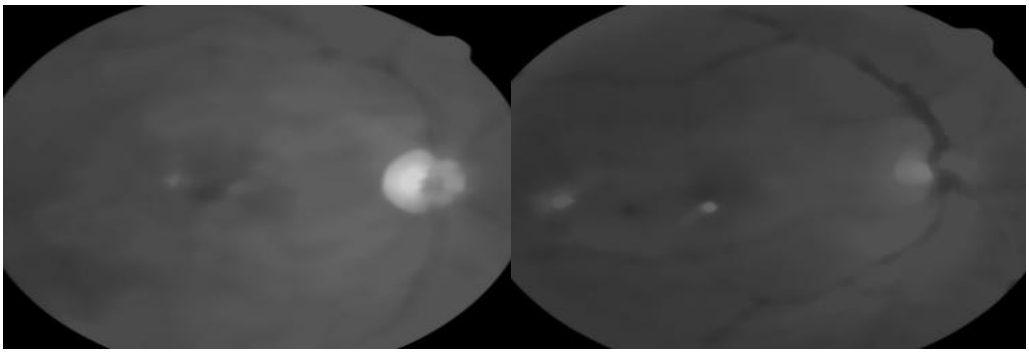

(e) (f)

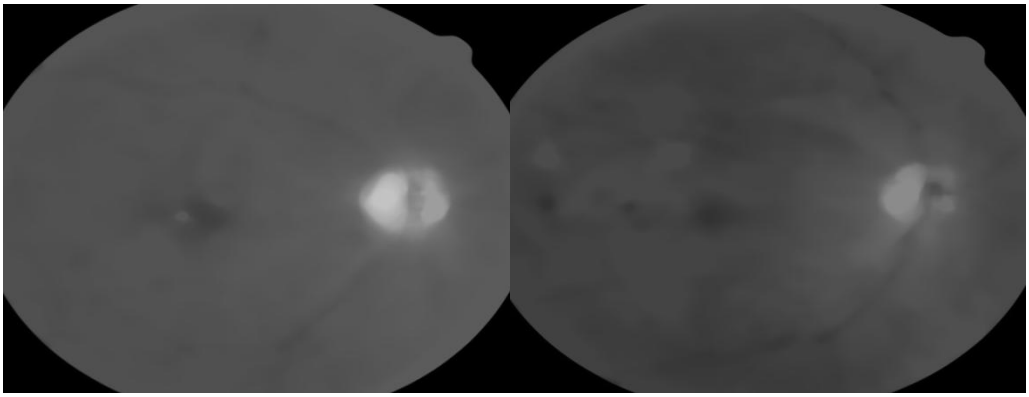

(g) (h)

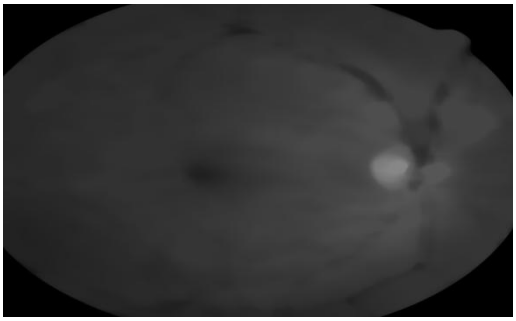

(i)

Figure4.4: a, b, c, d, e, f, g, h, i show the retinal image after morphological operation

IV) IMAGE NORMALIZATION

In image normalization technique, the dark and bright region is classified shown in figure 7(a, b, c, d, e, f, g, h, i). Histogram of normalized image shown all pixels centered at zero shown in figure 8(a, b, c, d, e, f, g, h, i). The normalized image is called exudate candidate detection.

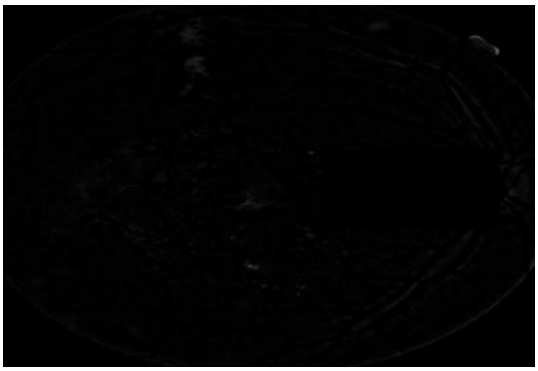

(a)

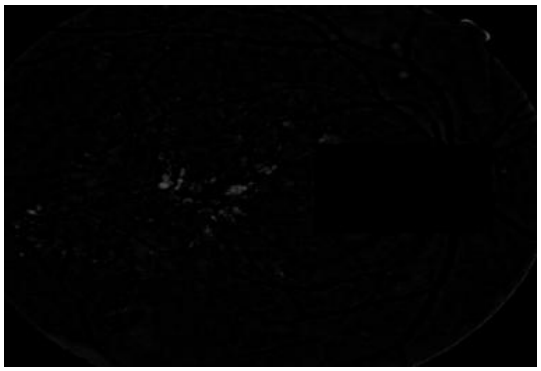

(b)

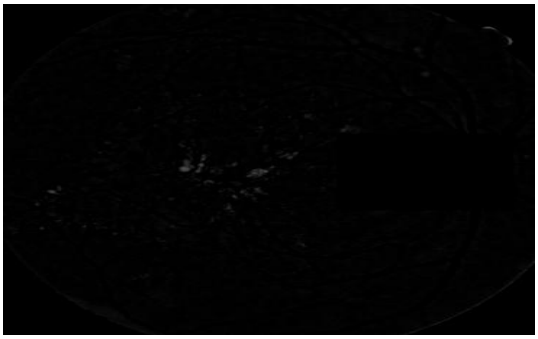

(c)

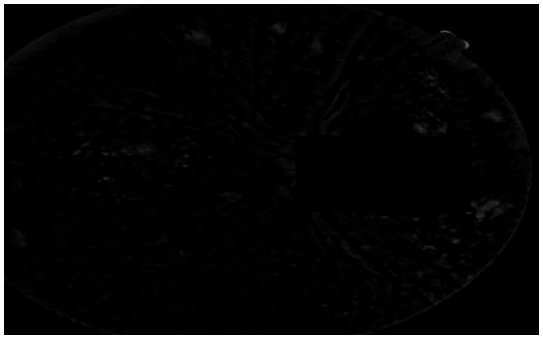

(d)

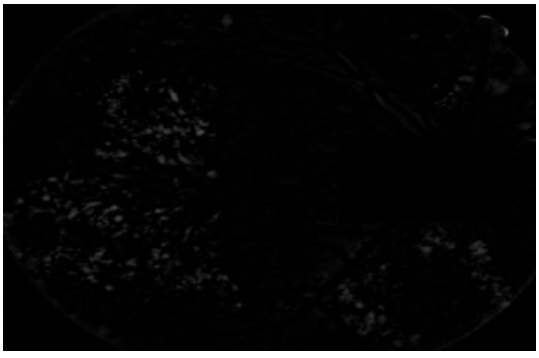

(e)

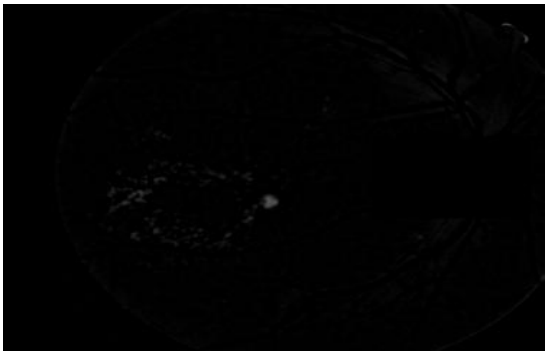

(f)

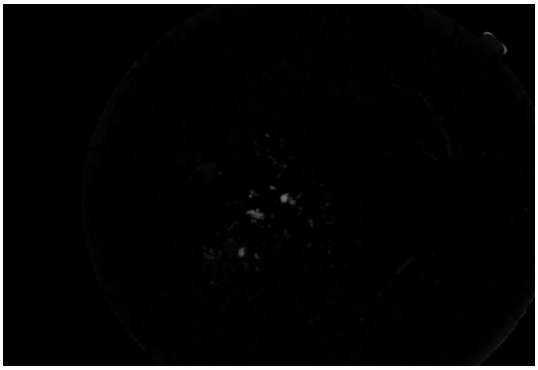

(g)

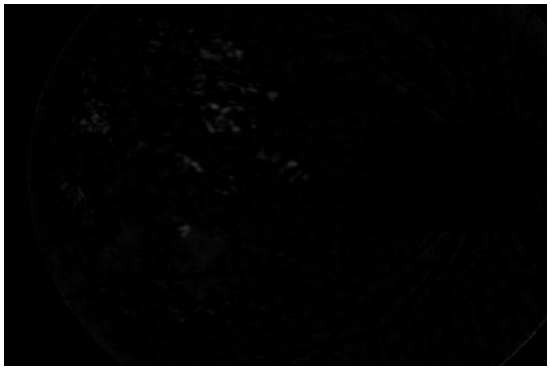

(h)

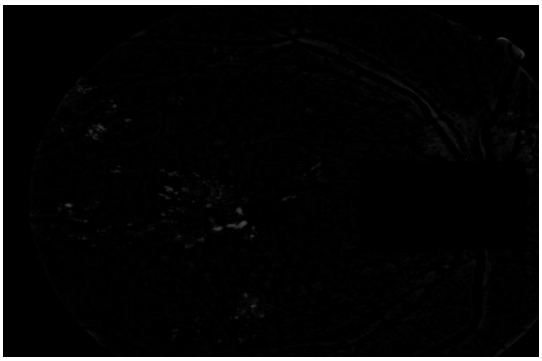

(i)

Figure4.5:a, b, c, d, e, f, g, h, i show the retinal image after image normalization

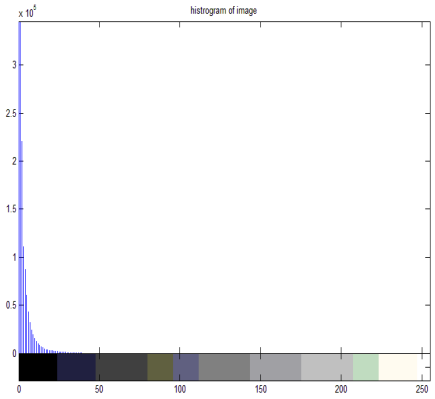

(a)

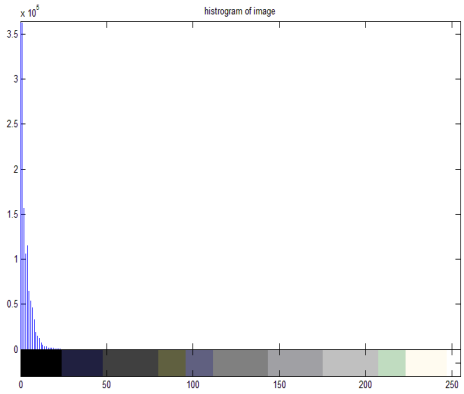

(b)

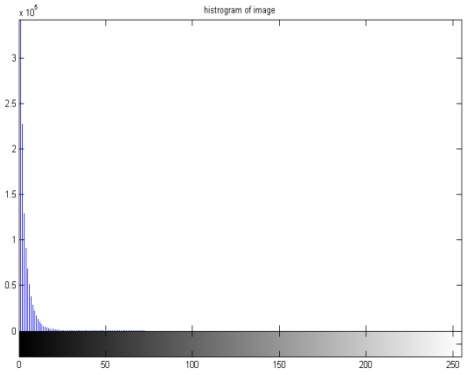

(c)

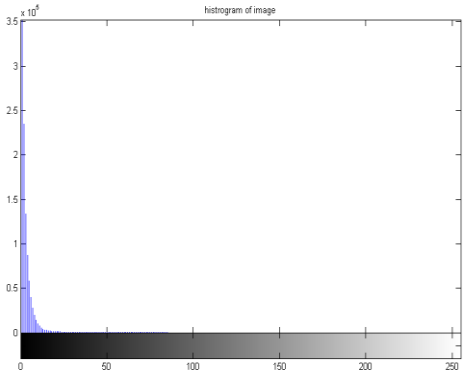

(d)

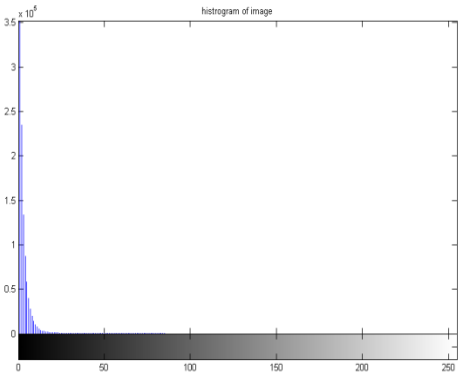

(e)

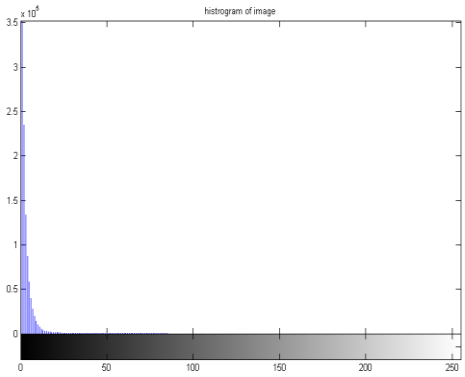

(f)

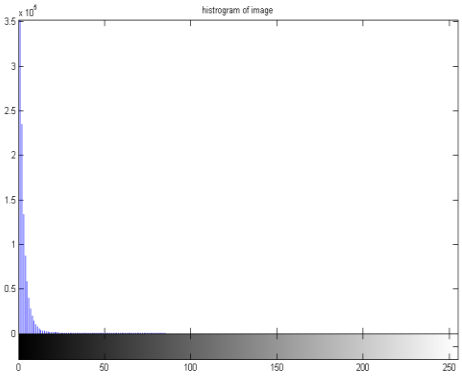

(g)

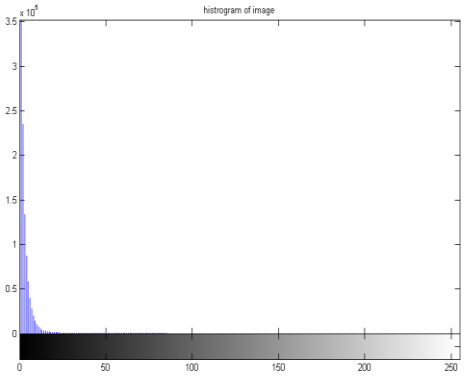

(h)

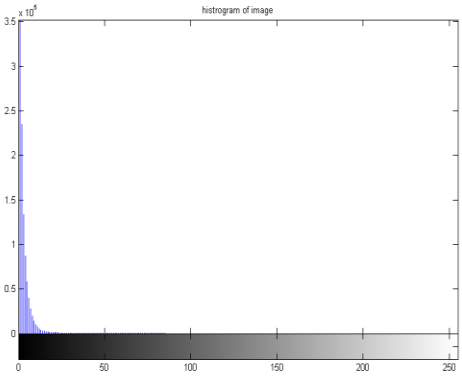

(i)

Figure4.6: a, b, c, d, e, f, g, h, i show the histogram of normalized image

V) EDGE DETECTION AND GLOBAL THRESHOLDING:

After image normalization we want to detect the external edge of the exudates candidate region, Using Kirsch's edge detection. Kirsch's operator is non-linear edge detector that find maximum edge strength in few predetermine direction. The operator takes a single kernel mask and rotates it in 45° increment through all compass direction. The edge magnitude of the kirsch operator is calculated as the maximum magnitude across all direction, and the resultant image is shown in figure 9(a, b, c, d, e, f, g, h, i).

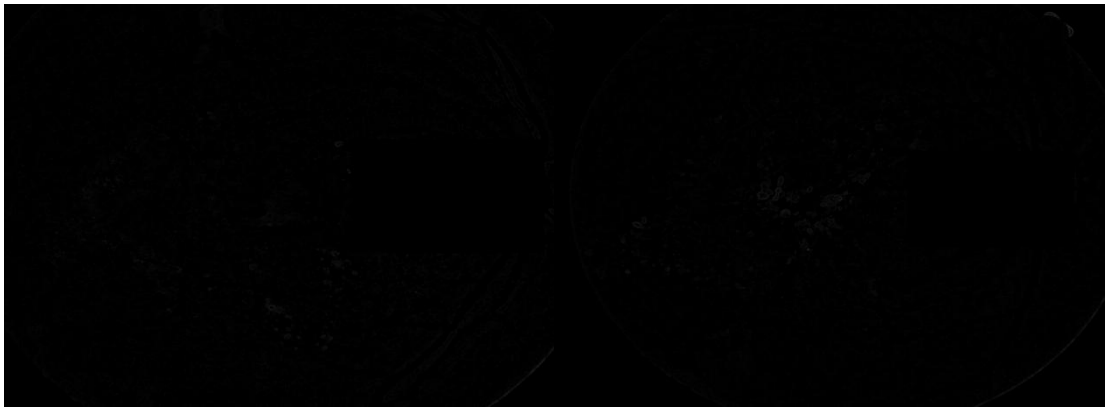

(a) (b)

(c) (d)

(e) (f)

(g) (h)

(i)

Figure4.7: a, b, c ,d, e, f, g, h, i show the edge detection

Converting the intensity image to binary image global thresholding is used intensity value lies in the range [0 1] .this level is called normalized intensity value. Then threshold to minimize the

intra class variance of the black and white pixels. Final exudates segmented image is shown in figure 10(a, b, c, d, e, f, g, h, i).

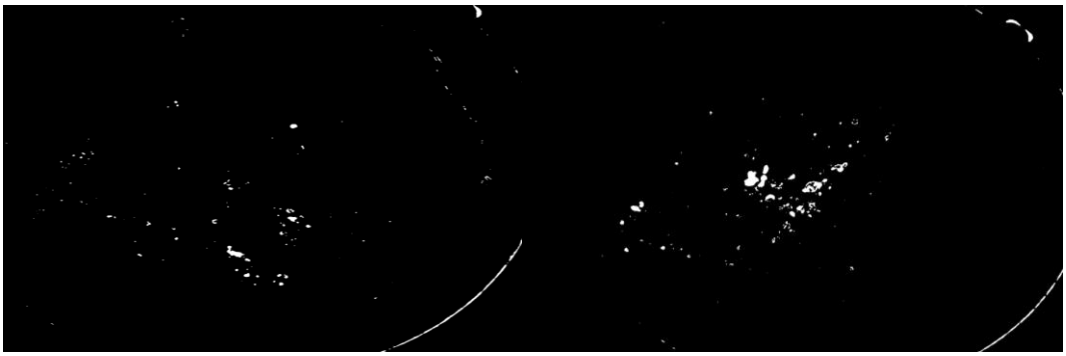

(a) (b)

(c) (d)

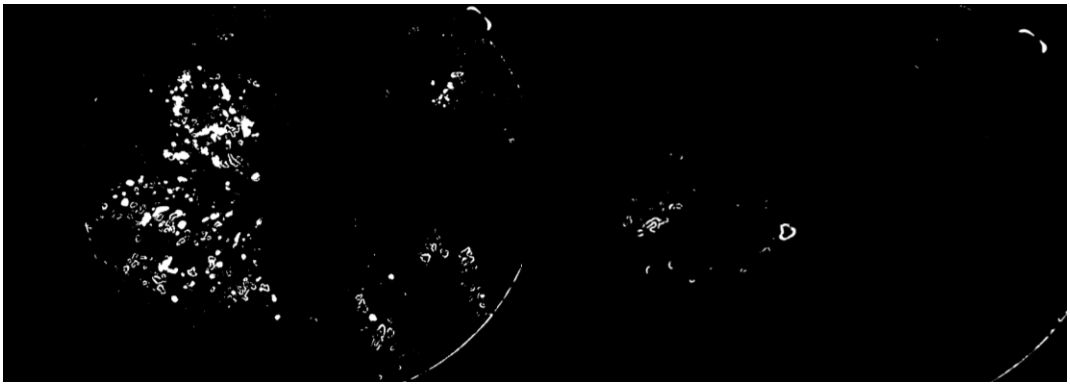

(e) (f)

(g) (h)

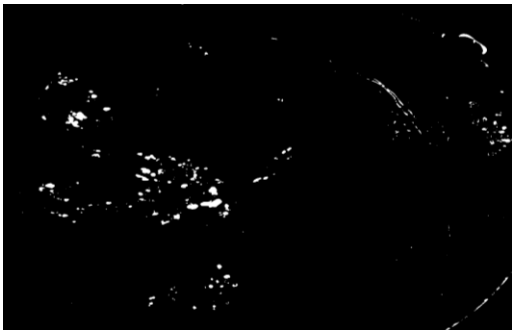

(i)

Figure4.8:a, b, c, d, e, f, g, h, i Show the candidate exudates detection

VI) FEATURE EXTRACTION:

The GLCM feature of exudates and non-exudates segmented region of the image is extracted. The size of the exudates and non-exudates region is equal. The segmented region of exudates and non-exudates regional size is (10x10) pixel.

The randomly select the slice of 42 exudates and 40 non-exudates region from 9 different retinal fundus images. And find the mean ± variance of GLCM properties like contrast, correlation, energy and homogeneity of exudates and non-exudates regions.

Table2

Shown that different cropped region of exudates and non-exudates of 9 different retinal fundus images for extraction of feature of that region

Images	Exudates cropped region	Non-exudates cropped region
Image 1		
Image 2		
Image 3		
Image 4		
Image 5		
Image6		
Image 7		
		
		
		
Image 8		
Image 9		
		

The GLCM Feature extraction like Contrast, Correlation, Energy, Homogeneity of all the input of retinal fundus image as show in the Appendix-1

Table3

GLCM feature values in terms of mean ± variance

Mean±Variance	Contrast	Correlation	Energy	Homogeneity
Exudates	0.1041±0.0032	0.7652±0.0245	0.4898±0.0187	0.9591±0.0008
Non-exudates	0.1825±0.0156	0.3329±0.0334	0.6031±0.0524	0.9087±0.0038

The GLCM Feature like Contrast, Correlation, Energy, Homogeneity of Exudates as well as Non-exudates region Mean ± Variance as shown in the Appendix-2.

VII) SVM CLASSIFIER:

In the proposed work, 82 slices of images chosen randomly from 9 retinal fundus images were chosen randomly feature is extracted and its classification was obtained. SVM classifier are separately contrast feature set. The SVM structure depends on the training set and testing set from feature like area, contrast, correlation, and homogeneity are given as input to SVM. To train the network 82 slice of image in 9 retinal fundus statistical features is loaded. Which are, contrast, correlation, energy, and homogeneity of retinal image from the workspace or from file. There are 17 images of testing for exudates region and corresponding 15 testing image for Non-exudates region .The computational result are presented

Table4

Confusion matrix for exudates classification

Parameter	Segmented exudates
TP	15
FP	0
FN	2
TN	15

The performance of proposed system is measured using sensitivity, specificity, PPV, accuracy and MCC. Sensitivity is true positive rate. Specificity is true negative rate. Table 3 clearly shows that the designed computer aided system to diagnose AMD out performs the other existing methods in terms of its performance by measuring Sensitivity, specificity, PPV, Accuracy, MCC.

Table 5

Comparative performance evolution of proposed computer aided diagnostic system with existing method

Method	Sensitivity	Specificity	PPV	Accuracy	MCC
Wang et al [18]	-	70	-	-	-
Walter et al [12]	92.74	100	92.39	-	-
Ahmed et al [22]	96.7	100	94.9	-	-
Osareh et al [21]	93	94.1	-	93.4	-
Akram et al [5]	-	-	-	-	94.73
Proposed method	88.23	100	100	93.75	88.23

Table6

Bar diagram of performance

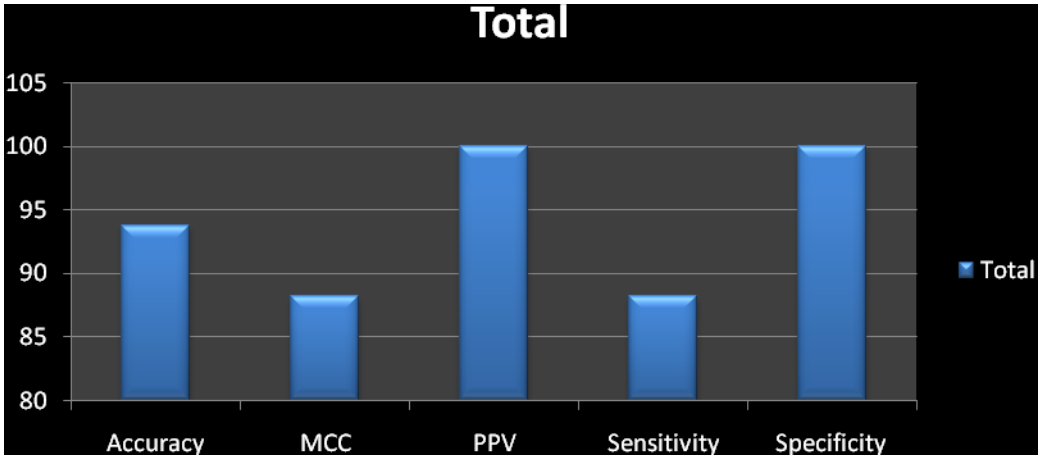

CHAPTER5

CONCLUSIONS

The proposed work presents the designing of computer aided diagnostic system for identification of exudates in retinal fundus images. System consists of three phases these are candidate exudates detection, feature extraction, and classification. The bright region is enhanced and segmented using morphological reconstruction, image normalization and global thresholding. Normalization procedure gives a substantial computational advantage to our method. The median filter and morphological reconstruction gives good contrast of foreground image. Feature set of each candidate region is formed using different properties of exudate and non-exudate region. We implemented a SVM based classifier to divide the region into exudate and non-exudate regions. The results demonstrated that the proposed system can be used in computer aided diagnosis system for DR as it identified and detected exudates with high accuracies.

REFERENCES

[1] D. E. Singer, D. M. Nathan, H. A. Fogel, and A. P. Schachat, "Screening for diabetic retinopathy." Ann Intern Med, vol. 116, no. 8, P: 660–671, 1992.

[2] M. D. Abramoff, M. Niemeijer, M. S. A. Suttorp-Schulten, M. A. Viergever, S. R. Russell, and B. van Ginneken, "Evaluation of a system for automatic detection of diabetic retinopathy from color fundus photographs in a large population of patients with diabetes." Diabetes Care, vol. 31, no. 2, P: 193–198, 2008.

[3] S. Philip, A. D. Fleming, K. A. Goatman, S. Fonseca, P. McNamee, G. S. Scotland, G. J. Prescott, P. F. Sharp, and J. A. Olson, "The efficacy of automated "disease/no disease" grading for diabetic retinopathy in a systematic screening programme." Br J Ophthalmol, vol. 91, no. 11, P: 1512–1517, 2007.

[4] M.D. Abramoff, M.K. Garvin, Sonka, M, "Retinal Imaging and Image Analysis," IEEE reviews in Biomedical Engineering, vol.3, P:169, 210.

[5] M. U. Akram and S. A. Khan, "Automated detection of dark and bright lesions in retinal images for early detection of diabetic retinopathy", Journal of Medical System, vol.36, no.5, P:3151-3162, 2011.

[6] A. Tariq, M. U. Akram, A. Shaukat, S. A. Khan, "Automated Detection and Grading of Diabetic Maculopathy in Digital Retinal Images", Journal of Digital Imaging, vol. 26, no. 4, P: 803-812, 2013.

[7] M. U. Akram, A. Tariq, M. A. Anjum, M. Y. Javed, "Automated Detection of Exudates in Colored Retinal Images for Diagnosis of Diabetic Retinopathy", OSA Journal of Applied Optics, vol. 51 no. 20, P: 4858-486, 2012.

[8] R. Phillips, J. Forrester, and P. Sharp, “Automated detection and quantification of retinal exudates, ” Graefes Arch Clin Exp Ophthalmol, vol. 231, no. 2, P: 90–94, 1993.

[9] C. Sinthanayothin, J. F. Boyce, T. H. Williamson, H. L. Cook, E. Mensah, S. Lal, and D. Usher, “Automated detection of diabetic retinopathy on digital fundus images,” Diabetic Medicine, vol. 19, no. 2, P: 105–112, 2002.

[10] H. Li and O. Chutatape, “Automated feature extraction in color retinal images by a model based approach,” IEEE Transactions on Biomedical Engineering, vol. 51, no. 2, P: 246–254, 2004

[11] T. Walter, J. K. Klein, P. Massin, and A. Erginay, “A contribution of image processing to the diagnosis of diabetic retinopathy–detection of exudates in color fundus images of the human retina.” IEEE Transactions on Medical Imaging, vol. 21, no. 10, P: 1236–1243, 2002.

[12] A. Sopharak, B. Uyyanonvara, S. Barman, and T. H. Williamson, “Automatic detection of diabetic retinopathy exudates from non-dilated retinal images using mathematical morphology methods.” Computerized Medical Imaging and Graphics, vol. 32, no. 8, P: 720–727, 2008.

[13] D. Mittal, V. kumar, S. C. Saxena, N.Khandelwal, ”Neural networks based focal liver diagnosis using ultrasound images,”Computerized Medical Imaging and Graphics, vol.35,no-4,P:135-323, 2011.

[14] K. Kumari, D. Mittal, ”Automated Drusen Detection Technique for Age-Related Macular Degeneration” Society for science and education, united kingdom,vol.2, P:19-26, 2015.

[15] R. Phillips, T. Spencer, P. Ross, P. Sharp, and J. Forrester, “Quantification of diabetic maculopathy by digital imaging of the fundus,” Eye, vol. 5, P: 130–137, 1991.

[16] R. Phillips, J. Forrester, and P. Sharp, "Automated detection and quantification of retinal exudates," Graefe's Arch. Clin. Exp. Ophthalmol., vol. 231, P: 90–94, 1993.

[17] B. Ege, O. Larsen, and O. Hejlesen, "Detection of abnormalities in retinal images using digital image analysis," in Proc. 11th Scand. Conf. Image Process., vol. 13, P: 833–840, 2009.

[18] H. Wang, H. Hsu, K. Goh, and M. Lee, "An effective approach to detect lesions in retinal images," in Proc. IEEE Conf. Comput. Vis. Pattern Recogn., Hilton Head Island, vol. 2, P: 181–187, 2000.

[19] M. Niemeijer, B. V. Ginneken, S. R. Russell, M. Suttorp, and M. D. Abramoff, "Automated detection and differentiation of drusen, exudates and cotton-wool spots in digital color fundus photographs for diabetic retinopathy diagnosis," Invest. Ophthalmol. Vis. Sci., vol. 48, P: 2260–2267, 2007

[20] M. Goldbaum, S. Moezzi, A. Taylor, and S. Chatterjee, "Automated diagnosis and image understanding with object extraction, object classification and inferencing in retinal images," in Proc. IEEE Int. Conf. Image Process., Lausanne, Switzerland, vol. 3, P: 695–698, 1996.

[21] Alireza O., B. Shadgar and R. Markham, "A Computational-Intelligence- Based Approach for Detection of Exudates in Diabetic Retinopathy Images", IEEE Trans on Information Tech in Biomedicine, vol. 13, No.4, P: 535-545, 2009.

[22] Ahmed Wasif Reza, C. Eswaran, Subhas Hati, "Automatic Tracing of Optic Disc and Exudates from Color Fundus Images Using Fixed and Variable Thresholds", Journal of Medical Systems, vol. 33, P: 7380, 2009

[23] S. Chugh, J Kaur,and D. mittal,"Exudates segmentation in retinal fundus image for detection of Diabetic retinopathy", IJERT,vol.3,2014. P:673-677.

[24] Methods to evaluate segmentation and indexing techniques in the field of retinal ophtalmology. [Online]. Available: http://messidor.crihan.fr

[25] L. Giancardo, M. Abramoff, E. Chaum, T. Karnowski, F. Meriaudeau, and K. Tobin, "Elliptical local vessel density: a fast and robust quality metric for retinal images," in Conf. of the IEEE EMBS, 2008.

[26] L. Giancardo," Quality Assessment of Retinal Fundus Images using ELVD". IN-TECH, 2010, ch. New Developments in Biomedical Engineering, P: 201–224, 2010.

[27] D. Mittal, V.Kumar, S.C.saxena, N. khandewal and N. kalra'' Enhancement of the ultrasound images by modified anisotropic diffusion method".Med. Biol.Engg. computer., vol.48, no-12, P:1281-1291, 2010

[28] L. Vincent, "Morphological grayscale reconstruction in image analysis: applications and efficient algorithms," IEEE Journal of Image Processing, vol. 2, no. 2, P: 176–201,1993

[29] A. D. Fleming, S. Philip, K. A. Goatman, J. A. Olson, and P. F. Sharp,"Automated microaneurysm detection using local contrast normalization and local vessel detection," IEEE Transactions on Medical Imaging, vol. 25, no. 9, P: 1223–1232, 2006

[30] C. I. Sanchez, M. Garca, A. Mayo, M. I. Lopez, and R. Hornero, "Retinal image analysis based on mixture models to detect hard exudates." Medical Image Analysis, vol. 13, no. 4, P: 650–658, 2009

[31] M. Niemeijer, B. van Ginneken, J. Staal, M. S. A. Suttorp-Schulten, and M. D. Abramoff, "Automatic detection of red lesions in digital color fundus photographs," IEEE Trans Med Imag, vol. 24, no. 5, P: 584– 592, 2005

[32] J. Kaur, D. Mittal ” Segmentation and Measurement of Exudates in Fundus Images of the Retina for Detection of Retinal Disease.”Society for science and education, united kingdom, vol.2., P:28-38, 2015

[33] R. A. Kirsch, “Computer determination of the constituent structure of biological images.” Computers and Biomedical Research, vol. 4, no. 3, P: 315–328, 1971

[34] K. Shanmugam, R. M. Haralick and I. H. Dinstein, “Textural features for image classification” IEEE Transactions on Systems, Man and Cybernetics 3, P: 610 – 621, 1973.

[35] R. Kohavi and F. Provost. Glossary of terms, Special Issue on “Applications, of Machine Learning and the Knowledge Discovery Process”, Journal of Machine Learning, vol. 30, P: 271–274, 1998

APPENDIX 1

The GLCM Feature Extraction of Green Channel of Retinal Fundus Image as Shown in Table:2

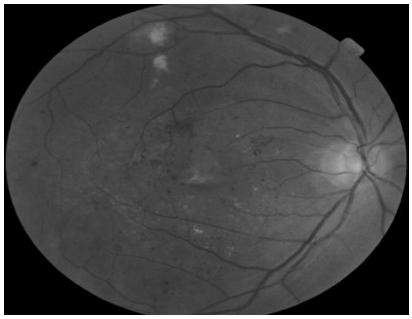

Figure5: Green channel of retinal fundus image 1

Table7
Cropped pixel location Area (10x10) with GLCM properties of Green channel of retinal fundus image 1

Pixel location of left below corner of cropped image	Contrast	Correlation	Energy	Homogeneity
934, 199	.2818	.3105	.3889	.8591
939, 217	.1455	.5859	.5245	.9273
935, 212	.1182	.6103	.5925	.9409
1082, 1038	.1818	.6326	.4188	.9091
702, 497	.1091	.3939	.7228	.9455
1647, 1071	.1909	.3455	.5538	.9045
887, 1243	.0091	.6621	.9641	.9955
1337, 1034	.2727	.4529	.3031	.8636

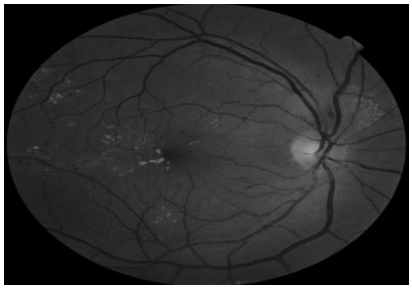

Figure6: Green channel of retinal fundus image 2

Table8
Cropped pixel location Area (10x10) with GLCM properties of green channel of retinal fundus image 2

Pixel location of left below corner of cropped image	Contrast	correlation	Energy	Homogeneity
951, 826	.1455	.8472	.2953	.9273
892, 838	.2091	.5936	.4021	.8955
945, 777	.1909	.6749	.3795	.9045
922, 827	.0455	.9168	.5385	.9773
1042, 452	.0727	.6511	.7241	.9636
1201, 1166	.4000	.1357	.2972	.8000
1188, 1164	.2545	.2304	.4795	.8727
1298, 1258	.0545	.0280	.8954	.9727

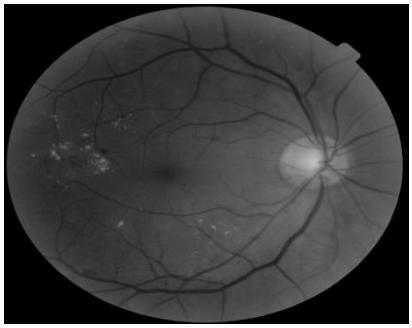

Figure7: Green channel of retinal fundus image 3

Table9

Cropped pixel location Area (10x10) with GLCM properties of green channel of retinal fundus image 3

Pixel location of left below corner of cropped image	Contrast	correlation	Energy	Homogeneity
586, 697	.0909	.7964	.4709	.9545
601, 722	.0364	.9272	.4651	.9818
756, 769	.0455	.8301	.6890	.9773
695, 618	.0727	.7122	.6944	.9636
1227, 849	.1091	.3939	.7228	.9455
901, 854	.2273	.3786	.4586	.8864
1195, 437	.0364	.3146	.9119	.9818
1345, 1102	.0455	.2622	.8950	.9773

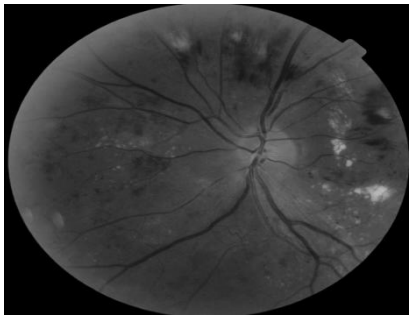

Figure8: Green channel of retinal fundus image 4

Table10
Cropped pixel location Area (10x10) with GLCM properties of green channel of retinal fundus image 4

Pixel location of left below corner of cropped image	Contrast	correlation	Energy	Homogeneity
1566, 693	.1455	.8384	.3643	.9273
1708, 875	.0545	.7806	.6998	.9727
1686, 897	.0636	.8303	.5654	.9682
1715, 900	.0636	.4992	.8133	.9682
937, 878	.1545	.6288	.4530	.9227
1252, 1168	.0455	.5215	.8616	.9773
605, 865	.1364	.5126	.6024	.9318
928, 956	.2727	.0457	.5159	.8636

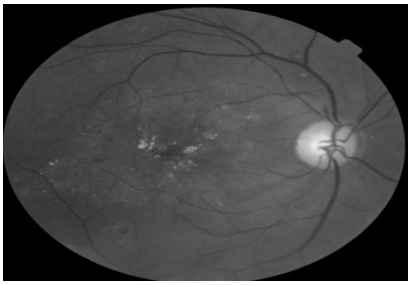

Figure9: Green channel of retinal fundus image 5

Table11
Cropped pixel location Area (10x10) with GLCM properties of green channel of retinal fundus image 5

Pixel location of left below corner of cropped image	Contrast	correlation	Energy	Homogeneity
893, 749	.1091	.8833	.3739	.9455
900, 731	.2273	.3619	.4682	.8864

590, 835	.0636	.8882	.4514	.9682
1058, 765	.0727	.7455	.6468	.9636
1334, 795	.2545	.2040	.4902	.8727
1293, 1111	.4273	.0492	.3059	.7864
1272, 995	.2909	.3295	.3598	.8545
994, 783	.1818	.3042	.5899	.9091

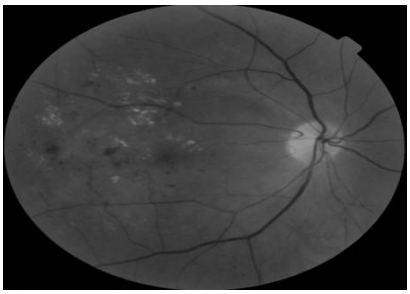

Figure10: Green channel of retinal fundus image 6

Table12
Cropped pixel location Area (10x10) with GLCM properties of green channel of retinal fundus image 6

Pixel location of left below corner of cropped image	Contrast	Correlation	Energy	Homogeneity
809, 896	.1091	.7643	.4400	.9455
1063, 726	.0273	.8874	.7314	.9864
900, 582	.0273	.9367	.5429	.9864
876, 568	.0818	.8746	.4333	.9591
1163, 582	.0364	.3146	.9119	.9818
1070, 1475	.0182	.6573	.9291	.9909
774, 760	.0545	.5956	.8136	.9727
1332, 893	.4455	.0922	.2623	.7773

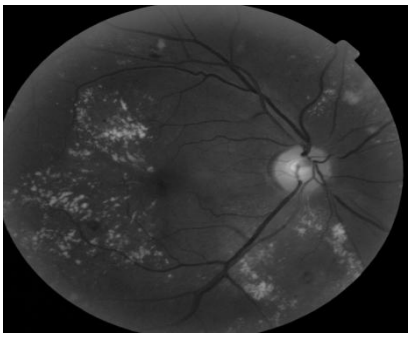

Figure11: Green channel of retinal fundus image 7

Table13
Cropped Pixel Location Area (10x10) with GLCM Properties of Green Channel of Retinal Fundus Image 7

Pixel location of left below corner of cropped image	Contrast	Correlation	Energy	Homogeneity
656, 852	.1091	.7536	.4880	.9455
724, 896	.1545	.8195	.3089	.9227
613, 880	.1455	.8134	.3310	.9273
828, 702	.1364	.8501	.3041	.9318
839, 610	.0909	.8732	.3924	.9545
916, 611	.1182	.8137	.4157	.9409
856, 490	.1000	.8109	.4861	.9500
651, 1064	.0727	.6984	.7092	.9636
1323, 1219	.1636	.5203	.5220	.9182
1294, 1182	.0545	.8896	.4544	.9727
1568, 987	.1091	.7190	.5145	.9455
1584, 1004	.1182	.5119	.6537	.9409
1296, 1184	.0636	.8260	.5747	.9682
1246, 529	.2727	.4107	.3388	.8636
1234, 665	.0636	.1890	.8619	.9682

1114, 769	.1091	.0846	.7836	.9455
1112, 1028	.2818	.1861	.4514	.8591
499, 647	.4000	.1527	.2879	.8000
1182, 177	.3182	.3572	.2881	.8409
1692, 739	.2818	.2820	.4051	.8591
479, 585	.1455	.1200	.7104	.9273
1194, 495	.3364	.3177	.2838	.8318

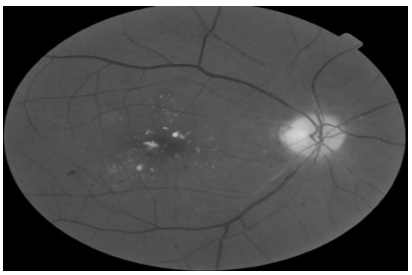

Figure12: Green channel of retinal fundus image 8

Table14

Cropped Pixel Location Area (10x10) with GLCM Properties of Green Channel of Retinal Fundus Image 8

Pixel location of left below corner of cropped image	Contrast	Correlation	Energy	Homogeneity
884, 907	.0909	.8487	.4007	.9545
1008, 739	.0636	.9760	.2261	.9682
932, 791	.0727	.9129	.3704	.9636
1222, 717	.0909	.1186	.8142	.9545

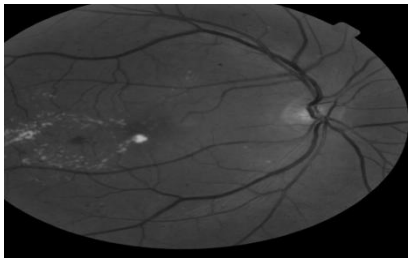

Figure13: Green channel of retinal fundus image 9

Table15

Cropped Pixel Location Area (10x10) with GLCM Properties of Green Channel of Retinal Fundus Image 9

Pixel location of left below corner of cropped image	Contrast	Correlation	Energy	Homogeneity
974, 861	.0364	.9641	.3797	.9818
632, 827	.0636	.8106	.6509	.9682
1066, 417	.0818	.2642	.8137	.9591
1062, 399	.2455	.2457	.4894	.8773
1064, 415	.0727	.2949	.8294	.9636
1054, 411	.2091	.1800	.5796	.8955
682, 491	.2273	.3939	.4994	.8864
1604, 1081	.0091	.6621	.9641	.9955

APPINDEX 2

The GLCM Feature Mean±Varience of Exudates and Non-exudates Region as Shown in Table: 3

Table16

Value of contrast, correlation, energy, and homogeneity of all 42 exudates region of 9 fundus images, and find the value of mean and variance

Count	Contrast	Correlation	Energy	Homogeneity
1	0.2818	0.3105	0.3889	0.8591
2	0.1455	0.5859	0.5245	0.9273
3	0.1182	0.6103	0.5925	0.9409
4	0.1818	0.6326	0.4188	0.9091
5	0.1455	0.8472	0.2953	0.9273
6	0.2091	0.5963	0.4021	0.8955
7	0.1909	0.6749	0.3795	0.9045
8	0.0455	0.9168	0.5385	0.9773
9	0.0909	0.7964	0.4709	0.9545
10	0.0364	0.9272	0.4651	0.9818
11	0.0455	0.8301	0.6890	0.9773
12	0.0727	0.7122	0.6944	0.9636
13	0.1455	0.8384	0.3643	0.9273
14	0.0545	0.7806	0.6998	0.9727
15	0.0636	0.8303	0.5654	0.9682
16	0.0636	0.4992	0.8133	0.9682
17	0.1091	0.8833	0.3739	0.9455
18	0.2273	0.3619	0.4682	0.8864
19	0.0636	0.8882	0.4514	0.9682
20	0.0727	0.7455	0.6468	0.9636
21	0.1091	0.7643	0.4400	0.9455
22	0.0273	0.8874	0.7314	0.9864

23	0.0273	0.9367	0.5429	0.9804
24	0.0818	0.8746	0.4333	0.9591
25	0.1091	0.7536	0.4880	0.9455
26	0.1545	0.8195	0.3089	0.9227
27	0.1455	0.8134	0.3310	0.9273
28	0.1364	0.8501	0.3041	0.9318
29	0.0909	0.8732	0.3924	0.9545
30	0.1182	0.8137	0.4157	0.9409
31	0.1000	0.8109	0.4861	0.9500
32	0.0727	0.6984	0.7092	0.9636
33	0.1636	0.5203	0.5220	0.9182
34	0.0545	0.8896	0.4544	0.9727
35	0.1091	0.7190	0.5145	0.9455
36	0.1182	0.5119	0.6537	0.9409
37	0.0636	0.8260	0.5747	0.9682
38	0.0909	0.8487	0.4007	0.4595
39	0.0636	0.9760	0.2261	0.9682
40	0.0727	0.9129	0.3704	0.9636
41	0.0364	0.9641	0.3797	0.9818
42	0.0636	0.8106	0.6509	0.9682
Sum	4.1818	32.14	19.5437	39.8078
Count	42	42	42	42
Average(mean)	0.099567	0.7652381	0.476676	0.947804764
Variance(s)	0.003737	0.02450033	0.024975	0.000803918

Table17

Value of contrast, correlation, energy, and homogeneity of all 42 non- exudates region of 9 fundus images, and find the value of mean and variance

Count	Contrast	Correlation	Energy	Homogeneity
1	0.1091	0.3939	0.7228	0.9455
2	0.1909	0.3455	0.5538	0.9045
3	0.0091	0.6621	0.9641	0.9955
4	0.2727	0.4529	0.3031	0.8636
5	0.0727	0.6511	0.7241	0.9636
6	0.4000	0.1357	0.2972	0.8000
7	0.2545	0.2304	0.4795	0.8727
8	0.1091	0.5825	0.6415	0.9455
9	0.1091	0.3939	0.7228	0.9455
10	0.2273	0.3786	0.4586	0.8864
11	0.0364	0.3146	0.9119	0.9818
12	0.0455	0.2622	0.8950	0.9773
13	0.1545	0.6288	0.4530	0.9227
14	0.0455	0.5215	0.8616	0.9773
15	0.1364	0.5126	0.6024	0.9318
16	0.2727	0.0457	0.5159	0.8636
17	0.2545	0.2040	0.4902	0.8727
18	0.4273	0.0492	0.3059	0.7864
19	0.2909	0.3295	0.3598	0.8545
20	0.1818	0.3042	0.5899	0.9091
21	0.0364	0.3146	0.9119	0.9818
22	0.0182	0.6573	0.9291	0.9909
23	0.0545	0.5956	0.8136	0.9727
24	0.4455	0.0922	0.2623	0.7773
25	0.2727	0.4107	0.3388	0.8636
26	0.0636	0.1890	0.8619	0.9682

27	0.1091	0.0846	0.7836	0.9455
28	0.2818	0.1861	0.4514	0.8591
29	0.4000	0.1527	0.2879	0.8000
30	0.3182	0.3572	0.2881	0.8409
31	0.2818	0.2820	0.4051	0.8591
32	0.1455	0.1200	0.7104	0.9273
33	0.3364	0.3177	0.2877	0.8318
34	0.0909	0.1186	0.8142	0.9545
35	0.0818	0.2642	0.8137	0.9591
36	0.2455	0.2457	0.4894	0.8773
37	0.0727	0.2949	0.8294	0.9636
38	0.2091	0.1800	0.5796	0.8955
39	0.2273	0.3939	0.4494	0.8864
40	0.0091	0.6621	0.9641	0.9955
Sum	7.3001	13.318	24.1247	36.3501
Count	40	40	40	40
Average(mean)	0.182503	0.33295	0.603118	0.9087525
Variance(s)	0.015568	0.03347271	0.052463	0.003892528

APPINDEX 3

Matlab Programming to Detection of Exudates in Retinal Fundus Image

Programming No 1:

```
close all
clc
clear all
% santosh kumar mishra
% master of engineering, Electronic instrumentation and control engineering
% Electrical and instrumentation engineering department
% Thapar university, patiala (india)
%Designing of computer aided diagnostic system for the identification of exudates in retinal
fundus images
%load image and convert to Green channel
%show the green channel pixel location
%tyrgb is retinal image image notation
% ty is green channel image notation
tyrgb = imread('miriex13.tif');
ty=tyrgb(:,:,2);
red=tyrgb(:,:,1);
if sum(ty(:))>sum(red(:))
   disp('ty');
else
   disp('red')
end
figure; imshow(ty);title('green channel')
%imtool(ty)

%% apply a median  filter to remove noise.
% Add Noise
b = imnoise(ty,'salt & pepper',.01);
%figure;imshow(b)
% Apply medfilt2 function
% size 1/30 row of the tif image for better background estimation
tywf=medfilt2(ty,[50 50]);
%tywf=medfilt2(b,[73,73]);
%figure;
%subplot(1,1,1);imshow(ty);title('Original image')
imshow(uint8(tywf));title('Denoised image 1')
%rescale the image adaptively to enhance contrast without enhancing noise
%tywfb = adapthisteq(tywf);
%figure;imshow(uint8(tywfb));title('show tywfb')

bgmask=zeros(1449,2201);
```

```
%figure;imshow(bgmask);title('masked image')
%% apply back ground estimstion
for x=1:1449
   for y=1:2201
      if ty(x,y)<tywf(x,y)
         bgmask(x,y)=tywf(x,y);
      else
        bgmask(x,y)=ty(x,y);
      end
   end
end
 figure;imshow(uint8(bgmask));title('background estimation')
%figure;imshow(ty);title('aa')
% processing for morphological reconstruction
marker = imsubtract(tywf,10);
recon = imreconstruct(marker,tywf);
figure;imshow(recon);title('reconstruct image')
% processing for image normalization
reconn=imsubtract(ty,recon);
imshow(uint8(reconn));title('normalized image')
imhist(reconn);title('histrogram of normalized image')
%Masking of optical nerve as mature technique
for x=615:900
   for y=1250:1660
      reconn(x,y)=0;
   end
end
%%
%applying Kirsch's Templates
% detection of edges of the exudates region using Kirsch's method
h1=[5 -3 -3;
   5  0 -3;
   5 -3 -3]/15;
h2=[-3 -3 5;
   -3  0 5;
   -3 -3 5]/15;
h3=[-3 -3 -3;
    5  0 -3;
    5  5 -3]/15;
h4=[-3  5  5;
   -3  0  5;
   -3 -3 -3]/15;
h5=[-3 -3 -3;
   -3  0 -3;
    5  5  5]/15;
```

```
h6=[ 5  5  5;
   -3  0 -3;
   -3 -3 -3]/15;
h7=[-3 -3 -3;
   -3  0  5;
   -3  5  5]/15;
h8=[ 5  5 -3;
    5  0 -3;
   -3 -3 -3]/15;
%Spatial Filtering by Kirsch's Templates
t1=filter2(h1,reconn);

t2=filter2(h2,reconn);
t3=filter2(h3,reconn);
t4=filter2(h4,reconn);
t5=filter2(h5,reconn);
t6=filter2(h6,reconn);
t7=filter2(h7,reconn);
t8=filter2(h8,reconn);
p=size(reconn);
exudate=zeros(p(1),p(2));
temp=zeros(1,8);
threshold=4;

for x=1:p(1)
   for y=1:p(2)
      temp(1)=t1(x,y);temp(2)=t2(x,y);temp(3)=t3(x,y);temp(4)=t4(x,y);
      temp(5)=t5(x,y);temp(6)=t6(x,y);temp(7)=t7(x,y);temp(8)=t8(x,y);

      if (max(temp))>threshold
         exudate(x,y)=max(temp);
      end
   end
end
z = uint8(exudate);
figure;imshow(z);title('kirsch edge of exudates region ')
level = graythresh(z);
bw= im2bw(z,level);
w=fspecial('average',5);
fa=imfilter(bw,w);
%ta=graythresh(fa);
ga=im2bw(fa,level);
%figure;imshow(ga);title('vvv')
%bw = bwareaopen(ga, 50);
%figure; imshow(bw)
```

```
bw1=imfill(ga,'holes');
figure;imshow(bw1);title('exudates detection')
bwc1=imclearborder(bw1,8);
imwrite(bw1,'C:\Users\santtosh\Documents\PJ8.bmp','bmp');
imwrite(ty,'C:\Users\santtosh\Documents\PJ9.bmp','bmp');
imwrite(recon,'C:\Users\santtosh\Documents\PJ14.bmp','bmp');
imwrite(z,'C:\Users\santtosh\Documents\PJ10.bmp','bmp');
imwrite(tywf,'C:\Users\santtosh\Documents\pj11.bmp','bmp');
imwrite(uint8(bgmask),'C:\Users\santtosh\Documents\pj12.bmp','bmp');
imwrite(uint8(reconn),'C:\Users\santtosh\Documents\pj13.bmp','bmp');
```

Matlab Programming GLCM Feature Extraction of Green Channel of Retinal Fundus Images
Programming No2:

```
% %load image and convert to grayscale
tyrgb = imread('miriex21.tif');
ty=tyrgb(:,:,2);
red=tyrgb(:,:,1);
if sum(ty(:))>sum(red(:))
   disp('ty');
else
   disp('red')
end
figure; imshow(ty);title('green channel')
imtool(ty);
ty1=imcrop(ty,[774 760 10 10]);
%imtool(ty1);
imshow(ty1);title('im1e')
%glcm3=graycomatrix(ty1, 'offset', [0 1], 'Symmetric', true);
glcm4=graycomatrix(ty, 'offset', [0 1], 'Symmetric', true);
%GLCM2 = graycomatrix(ty1,'Offset',[2 0;0 2]);
stats = graycoprops(glcm4);
imwrite(ty1,'C:\Users\santtosh\Documents\crop.bmp','bmp');
imwrite(ty,'C:\Users\santtosh\Documents\PJ9.bmp','bmp');
```

Matlab Programming to SVM Classification of Exudates and Non- Exudates Region
Programming No 3:

```
clear
clc
close all

T=xlsread('selected_classification.xlsx',1,'BA2:BQ301');
C=xlsread('selected_classification.xlsx',1,'W2:W301');
```

```
test=xlsread('selected_classification.xlsx',1,'BA2:BQ301');
```